PHYSICAL REVIEW B VOLUME 27, NUMBER 8 15 APRIL 1983

Optical absorption from polarons in a model of polyacetylene

K. Fesser, A. R. Bishop, and D. K. Campbell
Theoretical Division and Center for Nonlinear Studies, Los Alamos National Laboratory, Los Alamos, New Mexico 87545
(Received 25 October 1982)

We present a theoretical calculation, within a continuum electron-phonon-coupled model, of the optical absorption due to polarons in polyacetylene [$(CH)_x$]. Our results can be applied to both *trans*- and *cis*-$(CH)_x$, as well as potentially to other polymers (polypyroles, polyparaphenylenes) in which polarons are present. We establish that the essential signature of polaron absorption is the existence of three separate absorption peaks in the gap with qualitatively different features. For *trans*-$(CH)_x$, we compare and contrast this structure with that from the kink solitons, which are expected to dominate the optical absorption at all but the lowest doping levels. For *cis*-$(CH)_x$ and related polymers, we discuss polaron (and multipolaron) absorption and the relation of polarons to possible excitons in these materials. Finally, we evaluate briefly the existing experimental situation regarding optical absorption in polyacetylene and indicate possible future experiments that could confirm the existence of polarons in $(CH)_x$ and similar polymers.

I. INTRODUCTION

The proposal[1-3] that kink solitons play a central role in determining the electronic properties of *trans*-$(CH)_x$ (polyacetylene) has provoked considerable theoretical and experimental study of the system.[4] One of the most persuasive confirmations of the basic theoretical picture[1,5,6] has come from measurements of optical absorption[7,8] as a function of *n*- or *p*-type—doping concentration. It has been argued[1,5,6] that doping preferentially induces charged kinks which (in the simplest model, exhibiting charge-conjugation symmetry) are associated with localized electronic states at the middle of the semiconductor energy-band gap of pristine $(CH)_x$. Overlaps between these levels produce a narrow impurity band at midgap. Thus a midgap peak is expected in the optical absorption with intensity proportional to the dopant concentration (at low concentration) and the same for *n*- or *p*-type doping. Furthermore, it is predicted that weight is removed essentially uniformly in frequency from the interband absorption. These basic features have indeed been observed.[7-9]

More recently a second variety of soliton, a *polaron*,[10-13] has been recognized in the same models predicting the kink soliton. The polaron is more familiar than the kink but no less important for several reasons. Most significantly, this polaron (or its close descendant) is far more generic than the kink since, as we explain in Sec. III, it does not require *degenerate* conformations as in *trans*-$(CH)_x$. Thus, with some modifications in individual cases, the basic polarons we describe here should be relevant to many conjugated polymers (e.g., polyparaphenylenes, polypyrole, and derivatives). In particular, doping will be predicted[14] to occur via polaron creation. In principle, the cis isomer of $(CH)_x$, lacking the degeneracy of the trans isomer, also falls into this category. However, in practice it seems probable that here doping results in inhomogeneous cis-trans isomerization in the dopant neighborhood. (But see Ref. 15 and Sec. V.) The essential topological difference between *trans*-$(CH)_x$ and *cis*-$(CH)_x$ (and most other conjugated polymers) should still be apparent in other experiments, e.g., photogeneration of carriers.[10,16] Even in *trans*-$(CH)_x$ single electrons or holes will create a polaron rather than a separated kink-antikink pair. Polarons will eventually recombine to form kink-antikink pairs, but at low doping levels both kinks and polarons can be anticipated.[14] Recent optical-absorption data[14,17] on electrochemically doped samples may support this position (see Sec. V).

Whereas the kink soliton is associated with a midgap localized state in the model adopted in this paper, the polaron is associated with *two* localized levels symmetrically distributed about midgap. We will find that this leads to at most three (depending on the level occupations) optical-absorption peaks below the interband threshold. The structures of, and weights in, these peaks show a number of striking and hitherto unexpected features which we describe in detail and trace to the underlying "charge-conjugation symmetry" (see Appendix) of our model. The absorption weights are quite different from naive expectations and should be specif-

ic experimental labels.

The remainder of this paper is organized as follows. In Sec. II we briefly review the discrete electron-phonon-coupled model[1] of *trans*-$(CH)_x$ and its continuum limit, with which we work exclusively; no significant quantitative effects of lattice discreteness are expected. Analytic results for kink and polaron defects are given. Finally, a generalization of the Hamiltonian[13] is introduced which models the unique ground-state situation relevant to, e.g., *cis*-$(CH)_x$. Possible polaron excitations are again given analytically. In Secs. III and IV we derive optical-absorption coefficients in the presence of all allowed kinks and polarons and show that a sum rule (which has been proven in complete generality elsewhere[18,19]) is satisfied in these cases. Important differences between the structures of the results for the two types of excitations are emphasized. A kink interpolates between two different ground states, and this topology has required very careful attention to boundary conditions in past literature. The polaron is always asymptotic to a single ground state and boundary conditions are not a difficulty; nevertheless, we find that the polaron calculations further illuminate the role of boundary conditions in the kink case. Section V contains a brief summary and a discussion of the experimental scenario and more general theory of polarons into which our calculations fit. A number of our calculations are algebraically complicated, but this detail is necessary to understand the relationship to earlier kink results.[7,18,20] Since we do not wish to dilute the interesting structure of the results, extensive calculational details are relegated to the Appendix.

II. MODEL HAMILTONIANS, KINKS, AND POLARONS

The simplest microscopic model of *trans*-$(CH)_x$ is the discrete Su-Schrieffer-Heeger (SSH) Hamiltonian[1]

$$H=-\sum_{n,s}[t_0+\alpha(u_n-u_{n+1})]\times[C_{ns}^{\dagger}C_{n+1,s}+\text{H.c.}]+\tfrac{1}{2}K\sum_n(u_n-u_{n+1})^2 . \tag{2.1}$$

Here $C_{ns}^{\dagger}$ creates an (π) electron of spin s at site n, and u_n is the displacement of the (CH) unit at the nth site from its undistorted position. In *trans*-$(CH)_x$ the hopping matrix element t_0 is $\simeq$2.5 eV, the electron-phonon coupling constant is $\alpha\simeq$4.1 eV/ Å, and the spring constant (from σ bonds) is $K\simeq$21 eV/Å^2. Appropriate to $(CH)_x$ [and lightly doped $(CH)_x$] we consider one conduction electron per (CH) unit, i.e., a half-filled band, in which case the Hamiltonian (2.1) is unstable to a strongly commensurate (Peierls) dimerization. Near this limit, intrinsic defects in the dimerized chain appear as kinks or polarons, both of which have been observed in numerical studies of (2.1).[10,11] We wish to use these in detail and for this purpose it is most revealing to work with a continuum limit of (2.1) introduced by several authors[3,21,22]:

$$H=\sum_s\int\frac{dy}{l}\left[\frac{\omega_Q^2}{2g^2}\Delta^2(y)+\psi_s^{\dagger}(y)[-iv_F\sigma_3\frac{\partial}{\partial y}+\Delta(y)\sigma_1]\psi_s(y)\right] . \tag{2.2}$$

Here, $\omega_Q^2/2g^2=K/4\alpha^2$, and $v_F=2lt_0$, where l is the (undistorted) lattice constant. The (staggered) lattice displacement is described by $\Delta(y)$ and the electron field by the two component spinor

$$\psi_s=\begin{bmatrix}U_s\\V_s\end{bmatrix} .$$

The electron spectrum is linearized around the Fermi energy. Henceforth we will suppress the spin index s unless we need to use it explicitly. The continuum limit (2.2) will be useful if kinks or polarons are extended over many lattice spacings. Fortunately, this is the case in $(CH)_x$.[1] We have omitted the lattice dynamics from (2.1) and (2.2). In the usual *adiabatic* theory this adds a lattice kinetic energy proportional to $\dot{\Delta}^2(y)$. In fact, dynamics for the nonlinear excitations below is poorly understood, certainly analytically, and we will concentrate here purely on static solutions.

Variation of H in (2.2) leads to the mean-field single-particle electron wave-function equations[21]

$$\begin{aligned}\epsilon_n U_{ns}(y)&=-iv_F\frac{\partial}{\partial y}U_{ns}(y)+\Delta(y)V_{ns}(y) ,\\ \epsilon_n V_{ns}(y)&=+iv_F\frac{\partial}{\partial y}V_{ns}(y)+\Delta(y)U_{ns}(y) ,\end{aligned} \tag{2.3}$$

and the self-consistent gap equation

$$\Delta(y)=\frac{-g^2}{\omega_Q^2}\sum_{n,s}[V_{ns}^*(y)U_{ns}(y)+U_{ns}^*(y)V_{ns}(y)] . \tag{2.4}$$

The summation in (2.4) is over all occupied electron states.

The continuum electron-phonon-coupled equations (2.3) have essentially the form of single-particle Dirac equations in the presence of a poten-

tial $\Delta(y)$. The partial soliton ("reflectionless potential") properties of these equations have been emphasized in our earlier publications[12,23] and have been appreciated to varying degrees in several different physical contexts where the *same* equations have arisen.[24,25] Important facts are briefly reviewed in the Appendix and are responsible for our ability to find *analytic*, closed-form expressions for several nontrivial solutions. We now recall a few of these solutions for use in Sec. III.

First, the infinite, even chain has a double-degenerate ground state described by

$$\Delta(y)=\pm\Delta_0=\pm W\exp(\lambda^{-1}) , \tag{2.5}$$

where $\lambda^{-1}=\pi v_F\omega_Q^2/2g^2$ and W is the undimerized tight-binding bandwidth $W=4t_0=2v_F/l$. These ground states describe two dimerized configurations, out of phase by one lattice spacing. The corresponding one-electron energy spectrum (ϵ_n) is

$$\epsilon(k)=\pm\epsilon_k=\pm(k^2v_F^2+\Delta_0^2)^{1/2} , \tag{2.6a}$$

with plane waves as associated wave functions:

$$\begin{aligned} f_+^v &\equiv U^v+iV^v \\ &=-N_D(k)e^{iky}(1+i)\gamma^*(k)=f_+^c , \\ f_-^v &\equiv U^v-iV^v \\ &=-N_D(k)e^{iky}(1-i)\gamma(k)=-f_-^c , \end{aligned} \tag{2.6b}$$

where

$$\gamma(k)=1-\frac{ikv_F}{\epsilon_k-\Delta_0} ,$$

$$N_D=\frac{1}{2\sqrt{L}}\left[\frac{\epsilon_k-\Delta_0}{\epsilon_k}\right]^{1/2} .$$

In (2.6b) we have introduced the functions $f_\pm$ which have some technical and interpretive convenience[21,22] (see Appendix). The notation c,v refers to conduction- $[\epsilon(k)\geq\Delta_0]$ and valence- $[\epsilon(k)\leq-\Delta_0]$ band states. The charge-conjugation (particle-hole) symmetry[18,21,22] of the Hamiltonian (2.2) leads to the relationships between f^c and f^v indicated in (2.6b), as is shown in the Appendix. The gap in the energy spectrum (2.6a) is $2\Delta_0$ with the Fermi energy at $\epsilon=0$ [see Fig. 1(a)]. In chemical terms one can visualize the Peierls-dimerized ground states as alternating single and double bonds [see Fig. 1(b)]. If we evaluate the total energy per unit length, E, for a *uniform* dimerization $\Delta(y)=\Delta$, we find $E=-\Delta^2(\frac{1}{2}+\ln|\Delta_0/\Delta|)$ (in the weak coupling limit),[26] which emphasizes the degenerate configurations $\Delta=\pm\Delta_0$ and the instability at $\Delta=0$, i.e., uniform bond lengths [see Fig. 1(b)].

The twofold ground-state degeneracy in *trans*-$(CH)_x$ means that stable "kink-soliton" (K) defects are possible; these correspond to static, finite-energy lattice-displacement configurations which interpolate between the degenerate ground states [see Fig. 2(a)]:

$$\begin{aligned} &\Delta_K(y)=\Delta_0\tanh(y/\xi_0) , \\ &\xi_0\equiv v_F/\Delta_0 . \end{aligned} \tag{2.7a}$$

There is clearly also an antikink ($\bar{K}$) soliton with $\Delta_{\bar{K}}(y)=-\Delta_K(y)$. Depending on boundary conditions and the number of carbon atoms,[1,18,27] the ground state itself may or may not contain a kink (antikink), but additional excitations will occur in $K\bar{K}$ *pairs* on long chains for obvious energetic reasons. The associated one-electron energy spec-

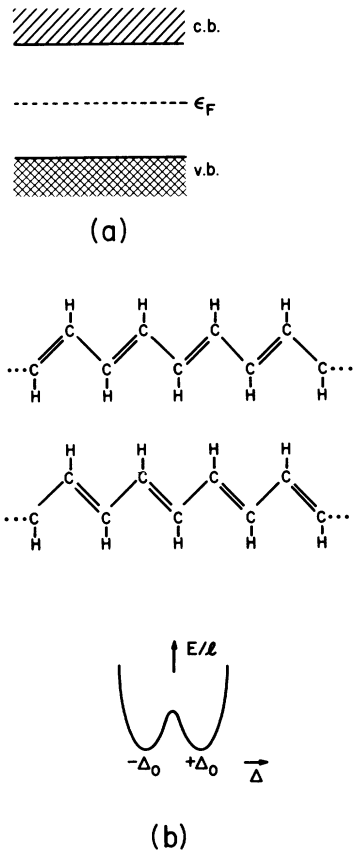

FIG. 1. (a) Energy spectrum of dimerized $(CH)_x$. The valence band (v.b.) is filled, the conduction band (c.b.) is empty, the Fermi level (ϵ_F) is at the middle of the gap. (b) The two schematic bond structures corresponding to the two degenerate ground states of *trans*-$(CH)_x$ and a schematic plot of the energy per unit length vs band-gap parameter Δ for spatially *uniform* Δ. Note the degeneracy between $\Delta=\pm\Delta_0$ and the local maximum (indicating instability) at $\Delta=0$.

trum [see Fig. 2(a)] consists of extended conduction- (c) and valence- (v) band states with the plane-wave dispersion as in the absence of a kink [i.e., (2.6a)], but with an additional "phase shift" determined from

$$f^v_{K+}(k)=N_K(k)e^{iky}[\tanh(y/\xi_0)-ik\xi_0] =f^c_{K+}(k)\ ,$$

where

$$f^v_{K-}(k)=iN_K(k)e^{iky}\epsilon_k/\Delta_0=-f^c_{K-}\ , \qquad N_K(k)=\frac{1}{\sqrt{L}}\frac{\Delta_0}{\epsilon_k}\ . \tag{2.7b}$$

Again charge-conjugation symmetry relates the valence- and conduction-band states, as indicated. The phase shift in (2.7b) with respect to (2.6b) is the only[28] effect on the extended states of the potential well presented by the pattern $\Delta_K(y)$ (see Appendix), but it has important consequences. In particular, the *density of states* is reduced (equally from the c and v bands because of charge-conjugation symmetry). These effects are discussed further in the Appendix, but in fact for an isolated kink (or antikink) exactly one-half state per spin, per band is lost and appears as a localized state at midgap, i.e., at the Fermi energy $\epsilon=\epsilon_0=0$ [see Fig. 2(a)], with associated wave function

$$f^0_+=\xi_0^{-1}\mathrm{sech}(y/\xi_0)\ , \qquad f^0_-=0\ . \tag{2.8}$$

The midgap state can be occupied by 0, 1, or 2 electrons giving kinks with the unusual spin-charge assignments[29] shown in Fig. 2(a). Explicit kink lattice (i.e., many $K\bar{K}$ pairs) solutions are also known analytically[22,30] (because of the same partial soliton character of the field equations) yielding a band of states centered around the Fermi energy with one state per kink removed from the extended states. We will work in a low defect density regime and do not need to consider the general kink lattice further here.

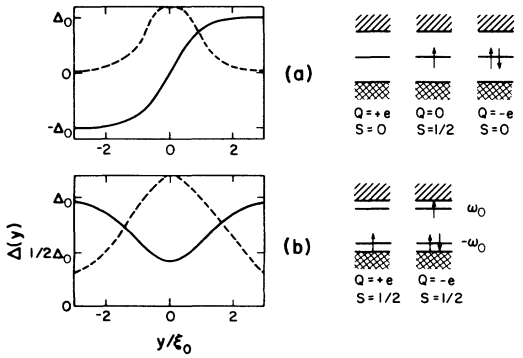

FIG. 2. Intrinsic defect states in *trans*-$(CH)_x$ and associated electronic levels: (a) kink, (b) polaron. Dashed lines indicate electron densities for localized states. $\xi_0=v_F/\Delta_0$, Q is the charge, S is the spin.

The most interesting solution to Eqs. (2.3) and (2.4) for our present purpose is the *polaron*, which we have described in detail elsewhere.[23] Although a highly nonperturbative strong coupling polaron, this solution has a most transparent analytic form: The polaron gap parameter is

$$\Delta_p(y)=\pm\Delta_0\mp K_0v_F\{\tanh[K_0(y+y_0)] -\tanh[K_0(y-y_0)]\}\ , \tag{2.9a}$$

with

$$\tanh(2K_0y_0)=K_0\xi_0\ . \tag{2.9b}$$

Evidently Δ_P describes a localized deviation about a single ground state ($\pm\Delta_0$), which will be important for *cis*-$(CH)_x$ below. Again the conduction- and valence-band dispersions are unchanged from the defect-free case (2.6a), but the wave functions are asymptotically phase shifted. Explicitly,

$$f^v_{P+}(k)=-N_P(k)e^{iky}(1+i)\gamma^*(k) \times\left[\frac{k}{K_0}+i\tanh[K_0(y-y_0)]\right] \tag{2.10a}$$

and

$$f^v_{P-}(k)=-N_P(k)e^{iky}(1-i)\gamma(k) \times\left[\frac{k}{K_0}+i\tanh[K_0(y+y_0)]\right]\ , \tag{2.10b}$$

where

$$N_P(k)=\frac{1}{2\sqrt{L}}\left[\frac{\epsilon_k-\Delta_0}{\epsilon_k}\right]^{1/2}\left[\frac{K_0^2}{k^2+K_0^2}\right]^{1/2}\ .$$

Again $f^c_{P+}=f^v_{P+}$ and $f^c_{P-}=-f^v_{P-}$. The phase shifts in (2.10) with respect to (2.6b) again imply a density-of-states reduction (see Appendix), now of one state per spin, per band, consistent with *two* localized one-electron eigenstates with energies in the gap at $\epsilon_\pm=\pm\omega_0$ where

$$\omega_0=(\Delta_0^2-K_0^2v_F^2)^{1/2}\ . \tag{2.11}$$

The symmetry about the Fermi energy is again a consequence of the charge-conjugation symmetry of (2.2). The corresponding wave functions are, for $\epsilon=\epsilon_+=+\omega_0$,

$$f_+^{+0}=N_P^0(1+i)\mathrm{sech}[K_0(y-y_0)]\ ,$$
$$f_-^{+0}=N_P^0(1-i)\mathrm{sech}[K_0(y+y_0)]\ , \tag{2.12}$$

where $N_P^0=\frac{1}{2}\sqrt{K_0}$ and, for $\epsilon=\epsilon_-=-\omega_0$, $f_+^{-0}=f_+^{+0}$ and $f_-^{-0}=-f_-^{+0}$. We emphasize that $\Delta_P(y)$ and the associated electron wave functions satisfy the electron part (2.3) of the continuum equations for *any* $K_0 v_F$ in $(0,\Delta_0)$.[31] However, the gap equation (2.4) is satisfied with a unique value for a given pair of localized level occupations $(n_+,n_-=0,1,2)$. The condition determining ω_0 is equivalent to minimizing the energy of the interacting electron-phonon system. Specifically, for *trans*-$(CH)_x$,

$$0=K_0 v_F\left[\frac{4}{\pi}\sin^{-1}(K_0\xi_0)-(n_+-n_-+2)\right]\ . \tag{2.13}$$

We see easily from (2.13) that only single-electron or single-hole polarons are nontrivial [$n_+=1$, $n_-=2$ or $n_+=0$, $n_-=1$, respectively; see Fig. 2(b)]. In these cases

$$K_0\xi_0=1/\sqrt{2}\ . \tag{2.14}$$

All other localized state occupations lead [see Eqs. (2.9b) and (2.13)] to infinitely separated $K\bar{K}$ pairs ($\omega_0=0$, $K_0\xi_0=1$, $y_0=\infty$), or the purely dimerized ground state ($\omega_0=\Delta_0$, $K_0\xi_0=0$, $y_0=\xi_0/2$), or linear combinations. Note that these are equilibrium configurations and do not rule out pinning of metastable configurations or tell us about relaxation time scales. The spin-charge assignments for polarons are entirely conventional [see Fig. 2(b)].

We emphasize the appealing simplicity of the polaron displacement pattern and electron wave functions. Comparing (2.7a) and (2.8) with (2.9a) and (2.12), it is natural to view the polaron as a $K\bar{K}$ bound state with separation $\sim 2y_0$ and kink shape (through K_0) coupled to y_0 [Eq. (2.9b)], i.e., a single-parameter family of configurations. It is then natural to expect bonding and antibonding localized gap states, but the simple sum and difference of isolated kink wave functions[22] ($\psi\equiv Ue^{iky}+iVe^{-iky}$) which one finds is more surprising. This simple structure is analytically very convenient and part of the beauty of the (partial) soliton properties of (2.3) and (2.4). It is also a little misleading, since the relative phase of the apparently free K and $\bar{K}$ is determined. This is also important in comparing with the polaron on a discrete lattice, since the phase of a kink determines whether it is centered on an even or odd atom (or somewhere between).[1,32]

Reasonable numbers for *trans*-$(CH)_x$ imply that both the localized kinks and polarons extend over many lattice spacings (15–20). Thus continuum theory should be good, and indeed several numerical simulations[10,11] of the discrete Hamiltonian (2.1) have found kink and polaron excitations in excellent agreement with (2.7a) and (2.9a).

To conclude this section we turn to the case of *cis*-$(CH)_x$, which allows us to display the possible excitations in a case that lacks ground-state degeneracy. We make use of a model suggested in this particular context by Brazovskii and Kirova,[13] whose consequences we have described in detail elsewhere.[12,33] The model has some extremely convenient analytic properties (which allow us to carry over the trans analysis directly), but more importantly it includes fundamental physical ingredients common to several conjugated polymers lacking degenerate ground states. In the case of *cis*-$(CH)_x$ there are two chemical structures corresponding to local energy minima but they do *not* have the same energy as in the trans isomer. The situation is depicted in Fig. 3. An obvious consequence of the lack of degeneracy is that *cis*-$(CH)_x$ (and similar polymers) *cannot* support stable *kink* excitations, since creating a $K\bar{K}$ pair separated by a distance d would cost energy $\sim d(\delta E/l)$, where $\delta E/l$ is the energy difference per bond between the stable and metastable phases. Clearly this linear "confinement" energy will prohibit K and $\bar{K}$ from becoming free. Of course, a confined $K\bar{K}$ pair is topologically reminiscent of a polaron [cf. Fig. 2(b)] so polarons *can* be

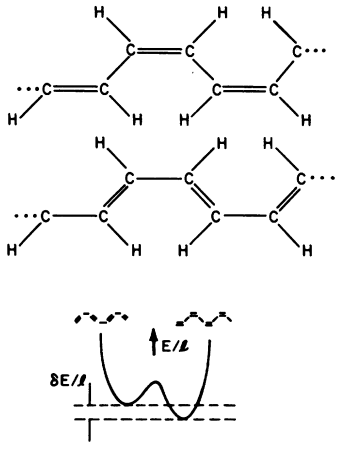

FIG. 3. Two schematic bond structures corresponding to the actual *cis*-$(CH)_x$ ground state (the cis-transoid configuration) and the metastable state (the trans-cisoid configuration) and a plot of the energy per unit length vs band-gap parameter Δ for spatially uniform Δ. Note that *cis*-$(CH)_x$ will have four (rather than two) one-electron bands, but we concentrate on the important band gap around the Fermi level.

anticipated in *cis*-$(CH)_x$.

To make these expectations explicit we adopt the ansatz through which the gap parameters can be written as[13]

$$\tilde{\Delta}(y)=\Delta_i(y)+\Delta_e \ , \tag{2.15}$$

where $\Delta_i(y)$ is sensitive to electron-phonon coupling (as for the trans isomer above) but Δ_e is a *constant* extrinsic component. One can motivate Δ_e in terms of σ-bond orbitals but *ab initio* calculations are difficult. With this simple ansatz, we easily find that the continuum adiabatic Hamiltonian (2.2) is modified as[13,34]

$$H_{\rm cis}=\int \frac{dy}{l}\left[\frac{\omega_Q^2}{2g^2}\Delta_i^2(y) + \psi^+(y)\left[-iv_F\sigma_3\frac{\partial}{\partial y}+\tilde{\Delta}(y)\sigma_1\right]\psi(y)\right] . \tag{2.16}$$

Of course, all the parameters in (2.16) will generally take different values from the corresponding ones for *trans*-$(CH)_x$ in (2.2) (see Sec. V). It follows from (2.16) that the mean-field electron equations for the isomer cis are *precisely the same* as for the trans isomer, i.e., (2.3), with $\Delta(y)$ replaced by $\tilde{\Delta}(y)$ (and appropriate parameter-value changes). Thus, with these replacements, the electron spectra and eigenfunctions are *precisely the same. Differences* from the trans one arise purely from the mean-field gap equation which, from (2.16), has entirely the structure of (2.4), the trans result, but with $\Delta(y)$ replaced by $\Delta_i(y)$ [*not* $\tilde{\Delta}(y)$]. This leads to different constraints on allowed solutions and on the location of bound-state eigenvalues $\pm\omega_0$. Specifically, (i) the ground state has the unique form $\tilde{\Delta}(y)=\tilde{\Delta}_0=\Delta_i^0+\Delta_e$, with $\Delta_0=W\exp(-1/\lambda)$ and $\Delta_e/\tilde{\Delta}_0=\lambda\ln(\tilde{\Delta}_0/\Delta_0)$; (ii) kink solutions do *not* satisfy the gap equation (as anticipated above); and (iii) the polaron profile (2.9a) [with $\Delta(y)\to\tilde{\Delta}(y)$] *does* satisfy the gap equation if K_0 (or ω_0) satisfies

$$0=K_0V_F\left[\frac{\pi}{4}(n_+-n_-+2)-\gamma K_0v_F/\omega_0 - \sin^{-1}(K_0v_F/\tilde{\Delta}_0)\right] . \tag{2.17}$$

Here $\gamma=\Delta_e/\lambda\tilde{\Delta}_0$. For $\gamma=0$, (2.17) coincides with (2.13) as it should. However, for $\gamma>0$, (2.17) supports nontrivial confined solutions for *all* occupations, n_+ and n_-, of the two electronic gap states. Reasonable estimates for *cis*-$(CH)_x$ probably place γ in the range 0.5—1.0, but for more general orientation and application we have plotted in Fig. 4 the dependence of $\omega_0/\tilde{\Delta}_0$ on γ for all values of (n_+-n_-) [from Eqs. (2.11) and (2.17)]. A more complete description of the various types of polarons is given in Ref. 34. Of particular interest here are the "bipolaron" solutions with $n_+=n_-=0,1,2$ (doubly negative, neutral, or doubly positive charge), which are unstable toward infinitely separated $K\bar{K}$ pairs ($\omega_0\to0$) in the trans case ($\gamma\to0$). This separation is prevented for $\gamma>0$ by a term in the total electron-phonon energy which is proportional to γ and the $K\bar{K}$ separation, precisely the confinement mechanism we anticipated above. Bipolarons are *energetically* preferred over isolated polarons, but with a larger size ($2y_0$) than each singly occupied polaron.

One of the main experimental interests in polarons or kinks [in *trans*-$(CH)_x$] is their preferred status as doping states. This status is based on equilibrium energy arguments. We will return to this and other experimental considerations in Sec. V, but we now have all the necessary information to calculate optical-absorption coefficients for the trans and cis models (2.2) and (2.16).

III. OPTICAL-ABSORPTION COEFFICIENTS: FORMAL RESULTS

In this section we present our results obtained for optical absorption in the presence of the types of *polarons* introduced in Sec. II. Technical details are given in the Appendix. Since comparison with results obtained elsewhere for kinks[7,18,20] will be helpful, we present some of these here also. In addition, the kink topology has been recognized to play an essential role in correct evaluations of, among other

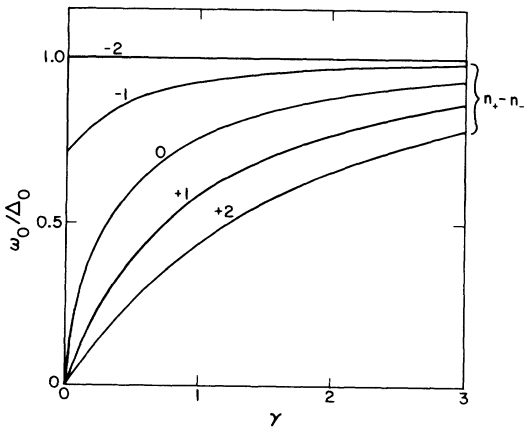

FIG. 4. Position of the polaron state ω_0 in the gap as a function of "confinement" parameter γ (see Sec. II) and occupation of the localized levels n_+,n_-. $\gamma=0$ corresponds to *trans*-$(CH)_x$.

quantities, the interband optical absorption: Diagonal transitions are specifically excluded by the relative density-of-states changes in the conduction and valence bands due to the boundary conditions in the presence of a kink.[18] A polaron, or any configuration with the topology of equal numbers of kinks and antikinks, presents different boundary conditions, and we will see how these modify the structure of the optical-absorption results.

As for previous kink calculations, we calculate the optical-absorption coefficient $\alpha(\omega)$ in a conventional linear-response dipole approximation:

$$\alpha(\omega)=\pi\frac{\xi_0}{L}\frac{\Delta_0}{\omega}A\sum_{\{1,2\}} n_{1,2}\,|M_{1,2}|^2\delta(\omega-\epsilon_1-\epsilon_2)\ , \tag{3.1}$$

where the summation is over all allowed transitions from eigenstate $|1\rangle$ to eigenstate $|2\rangle$ (with energies ϵ_1,ϵ_2), and the matrix element $M_{1,2}$ is

$$M_{1,2}=\langle 2|\sigma_3|1\rangle = \tfrac{1}{2}\int_{-L/2}^{L/2} dy[f_+^{2*}(y)f_-^1(y)+f_-^{2*}(y)f_+^1(y)]\ . \tag{3.2}$$

In (3.1)

$$A\equiv\frac{8\pi e^2\hbar|M_x|^2}{m^2cn\Delta_0}$$

(where e and m are the electron charge and mass, c the velocity of light, n the index of refraction, and M_x the momentum matrix element for the carbon π_z orbital),[7] and we have assumed normalization to unity on a line of length L, where L will be taken to infinity. The factor $n_{1,2}=0,1,2$ counts the number of possible transitions allowed by occupancy of the two states. The prefactor in (3.1) is written to isolate the characteristic scale ξ_0/L. This is convenient since we will be dealing with the effects of a single defect (kink or polaron), and therefore must account for all terms of order ξ_0/L. As explained in the Appendix these will come both from wave-function normalization and from density-of-states changes arising from phase shifts of the conduction- or valence-band states. With the prefactors in (3.1) the exact sum rule[18,19] for optical absorption takes the form

$$\int d\omega\,\alpha(\omega)=A\ . \tag{3.3}$$

In view of our description in Sec. II of the number and location of localized states in the gap for kinks and polarons, we can expect three classes of transitions for a kink and six for a polaron. These are denoted in Fig. 5, to which figure we refer for notation. As explained in the Appendix, charge-conjugation symmetry reduces the number of independent transitions to two for a kink and four for a polaron.

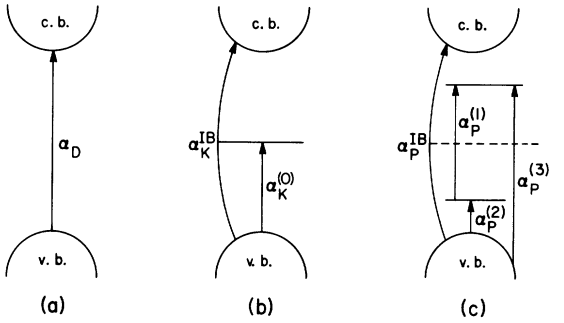

FIG. 5. Nomenclature for all possible different transitions: (a) dimerized chain; (b) single kink; (c) single polaron.

First, we summarize results for a single *kink*.[7,18,20] For a single transition [i.e., $n_{1,2}=1$ in (3.1)] from valence band to midgap or from midgap to conduction band [see Fig. 5(b)] the form of α which follows from (2.7b) and (2.8) in (3.2) is (see Appendix)

$$\alpha_K^{(0)}(\omega)=\frac{\pi^2}{4}A\frac{\xi_0}{L}(\omega^2-\Delta_0^2)^{-1/2}\times\operatorname{sech}^2\left[\frac{\pi}{2\Delta_0}(\omega^2-\Delta_0^2)^{1/2}\right]\ , \tag{3.4}$$

so that

$$\int_{\Delta_0}^{\infty}\alpha_K^{(0)}(\omega)d\omega=1.41\frac{\xi_0}{L}A\ . \tag{3.5}$$

From the matrix element symmetry (Appendix) we see that, independent of the midgap occupation, the total absorption from transitions between extended and localized states is twice that in (3.4) and (3.5). The interband absorption (IB) coefficient in the presence of a kink cannot be given analytically,[18] but for high frequency ($\omega\gtrsim 2.5\Delta_0$) weight is removed uniformly in ω with respect to the pure dimerized (D) case. Thus one has

$$\alpha_K^{IB}(\omega)\simeq\alpha_D(\omega)(1-2\xi_0/L)\ , \tag{3.6a}$$

where, by using (2.1) in (3.2),

$$\alpha_D(\omega)=A(2\Delta_0/\omega)^2(\omega^2-4\Delta_0^2)^{-1/2} \tag{3.6b}$$

is the interband absorption for the pure dimerized case. Numerically, the sum rule (3.3) is indeed found to be satisfied,[18] i.e.,

$$\int_{2\Delta_0}^{\infty} \alpha_K^{\mathrm{IB}}(\omega)d\omega = A(1-2.82\xi_0/L) \ . \tag{3.7}$$

The evaluation of (3.7) is interesting because of the absence of diagonal transitions, a result of the kink topology. This effect must be handled extremely carefully to avoid divergences. Below and in the Appendix we show how this differs from the polaron case and thereby gives a new perspective on existing kink calculations.[18]

Turning to results for the polaron, we consider first transitions involving the localized gap states[33] [see Fig. 5(c) for notation]:

(i) (Single) transition between localized levels. Using (2.12) in (3.2) we find

$$\alpha_P^{(1)}(\omega) = \pi A \frac{\xi_0}{L}\left[2\frac{\omega_0}{\Delta_0}\frac{y_0}{\xi_0}\right]^2 \frac{\Delta_0}{\omega}\delta(\omega-2\omega_0) \ , \tag{3.8}$$

$$\int \alpha_P^{(1)}(\omega)d\omega = \pi A \frac{\xi_0}{L}\frac{2\omega_0}{\Delta_0}\left[\frac{y_0}{\xi_0}\right]^2 .$$

(ii) Transitions between the valence band and the (singly occupied) $(-\omega_0)$ level [or $(+\omega_0)$ level to conduction band]. As explained in the Appendix, to find effects of order ξ_0/L in this case we do *not* have to include normalization or density-of-states corrections. Using (2.10) and (2.12) in (3.2) we find (Appendix)

$$\alpha_P^{(2)}(\omega) = A\frac{\xi_0}{L}\frac{\pi^2}{4}\frac{1}{K_0\xi_0}\frac{1}{X}\frac{\omega(\omega+\omega_0-\Delta_0)}{\Delta_0^3}\frac{1}{K_0^2\xi_0^2+X^2}\operatorname{sech}^2\left[\frac{\pi}{2}\frac{X}{K_0\xi_0}\right] \times\left[\sin\left[X\frac{y_0}{\xi_0}\right]+X[(1+X^2)^{1/2}-1]^{-1}\cos\left[X\frac{y_0}{\xi_0}\right]\right]^2 , \tag{3.9}$$

with

$$X=\left[\left[\frac{\omega+\omega_0}{\Delta_0}\right]^2-1\right]^{1/2} .$$

(iii) Transitions between the valence band and the (singly occupied) $(+\omega_0)$ level [or $(-\omega_0)$ level to conduction band]. Using (2.10) and (2.12) in (3.2) leads to (Appendix)

$$\alpha_P^{(2)}(\omega) = A\frac{\xi_0}{L}\frac{\pi^2}{4}\frac{1}{K_0\xi_0}\frac{1}{X}\frac{\omega(\omega+\omega_0-\Delta_0)}{\Delta_0^3}\frac{1}{K_0^2\xi_0^2+X^2}\operatorname{sech}^2\left[\frac{\pi}{2}\frac{X}{K_0\xi_0}\right] \times\left[\sin\left[X\frac{y_0}{\xi_0}\right]+X[(1+X^2)^{1/2}-1]^{-1}\cos\left[X\frac{y_0}{\xi_0}\right]\right]^2 , \tag{3.10}$$

with

$$Y=\left[\left[\frac{\omega-\omega_0}{\Delta_0}\right]^2-1\right]^{1/2} .$$

(iv) Interband transitions. In this case we *do* need to include both density-of-states and normalization corrections to order ξ_0/L, as explained in the Appendix. As we describe in detail in the Appendix it is convenient to split the matrix element $M_{kk'}$ (k and k' being wave vectors of states in the valence and conduction bands, respectively) into two terms; we call these $M_{kk'}^{\mathrm{diag}}$ and $M_{kk'}^{\mathrm{off\text{-}diag}}$. Contributions to the optical-absorption coefficient from diagonal transitions are found analytically. To order ξ_0/L

$$\alpha_P^{\mathrm{IB}}(\omega)(\mathrm{diag}) = \alpha_D(\omega)\left[1-\frac{\xi_0}{L}\frac{1}{K_0^2\xi_0^2+Z^2}[8K_0y_0(1+Z^2)-2K_0\xi_0]\right] , \tag{3.11}$$

with $Z=[(\omega/2\Delta)^2-1]^{1/2}$ and $\alpha_D(\omega)$ the absorption coefficient in the pure dimerized case [Eq. (3.6b)]. The integrated intensity from (3.11) is given by (including the factor of 2 from the two spin states)

$$\frac{2}{A}\int_{2\Delta}^{\infty}\alpha_P^{\mathrm{IB}}(\omega)(\mathrm{diag})d\omega = 1-\frac{\xi_0}{L}\left[\left[\frac{8y_0}{\xi_0}-\frac{2\Delta_0^2}{\omega_0^2}\right]\frac{\Delta_0}{\omega_0}\tan^{-1}\left[\frac{\omega_0}{K_0\Delta_0\xi_0}\right]+\frac{2K_0\xi_0}{(\omega_0/\Delta_0)^2}\right] . \tag{3.12}$$

As for the kink case (3.6), contributions from *off-diagonal* transitions can only be evaluated numerically. The

results of the necessary numerical double integration (over k,k') have been found [when taken together with (3.8)–(3.10) and (3.12)] to satisfy the sum rule (3.3) for *all* values of ω_0 in $(0,\Delta_0)$ and *all* localized level occupations. However, the structure of $M_{kk'}$ is worthy of closer analysis and comparison with the corresponding kink quantity. More details are given in the Appendix but we remark here on the following basic structure:

$$|M_{kk'}|^2=\mathcal{A}(k)\delta_{kk'}+\frac{1}{L^2}\mathcal{B}(k,k') , \tag{3.13}$$

representing the decomposition into the diagonal and off-diagonal components referred to above. $\mathcal{A}(k)\sim 1+O(1/L)$ leading to (3.12). The most interesting fact is that $\mathcal{B}(k,k')$ is *discontinuous* as $k\to k'$. This discontinuity follows directly from the integral

$$\lim_{L\to\infty}\int_{-L/2}^{L/2}dy\, e^{iy\Delta k}t_{\pm}=\begin{cases}\pm 2y_0 , & \Delta k=0\\ \dfrac{2i}{\Delta k}e^{\mp iy_0\Delta k}\dfrac{(\pi/2)(\Delta k/K_0)}{\sinh[(\pi/2)(\Delta k/K_0)]} , & \Delta k\neq 0\end{cases} \tag{3.14}$$

with $\Delta k=k'-k$ and $t_{\pm}=\tanh[K_0(y\pm y_0)]$. The relevance of this integral should be evident from the polaron forms for $f_{\pm}$ in (2.10) which are inserted in (3.2). We see that (3.14) diverges as $\Delta k\to 0$, implying an *infinite* discontinuity at $\Delta k=0$. In fact, for the polaron there are additional Δk factors in $\mathcal{B}(k,k')$ which control the divergence and render the discontinuity in $\mathcal{B}(k,k')$ *finite;* the explicit form is given in the Appendix. Since the discontinuity is finite, the necessary double integration on k and k' to evaluate $\alpha(\omega)$ is insensitive to the discontinuity to the order ξ_0/L in which we are working here.

It is instructive to contrast (3.13) and the discontinuity in $\mathcal{B}(k,k')$ with the situations in the pure dimerized and single-kink cases. In the former limit only diagonal transitions are allowed, i.e., $\mathcal{A}(k)\neq 0$, $\mathcal{B}(k,k')=0$. This result follows easily from (2.6) and (3.2) (see also the Appendix). By contrast, for a single kink (or antikink) only *off*-diagonal interband transitions survive[18]: Using (2.10) in (3.2) we find easily that $\mathcal{A}(k)=0$ and $\mathcal{B}(k,k')\neq 0$; $\mathcal{B}(k,k')$ involves the same integral (3.14) but with $y_0=0$. In the kink case there are no factors moderating the divergence as $\Delta k\to 0$. Consequently, $\mathcal{B}(k,k')$ has an *infinite* discontinuity as $\Delta k\to 0$, which *can* affect integration over (k,k') to $O(\xi_0/L)$. In this case it is necessary to recognize explicitly the quantization imposed on k and k' in a box of length L by the boundary conditions of a single kink.[18] Specifically,

$$kL=2n\pi+\tan^{-1}(k\xi_0)$$

for the conduction band, but

$$kL=(2n+1)\pi+\tan^{-1}(k\xi_0)$$

for the valence band (n is an integer). It follows that $\Delta k=0$ is *not* allowed and the incipient divergence in $\mathcal{B}(k,k')$ is avoided. The summation on Δk must be done carefully, but then the final summation (on, for example, k) can be safely taken in the continuum integral limit (including phase-shift effects on the density of states) as for the polaron calculation (Appendix). Physically, these differences between the kink and polaron calculations reflect the fact that for a single kink (or any configuration with the same topology) infinite portions (as $L\to\infty$) of the chain lie in each of the two ground states, whereas this is not so for the polaron (or other configurations of the same topology). Note that we always suppose $L\gg 2y_0$. Technically, the differences arise from the way phase shifts produce different relative wave-vector discretizations for the conduction and valence bands in the two cases: For the $K\bar{K}$ topology the allowed values of k in the conduction band satisfy $kL=(2n+2)\pi+$ phase shift. The 2π misregister between conduction and valence only affects transitions to $O(1/L)$ and therefore appears as a higher-order correction than we are keeping. However, the π misregister for a kink affects all transitions and must therefore be included. The same arguments lead us to conclude that any *finite* concentration of defects will create $O(1)$ corrections which must be included. These usually appear as explicit exclusions of states (one per kink, two per polaron) at the top of the valence band and at the bottom of the conduction band.

IV. OPTICAL-ABSORPTION COEFFICIENTS: ANALYSIS OF RESULTS AND LIMITS

Having summarized our results in (i)–(iv) of Sec. III we now focus on limiting behaviors, which are convenient and instructive checks, and on graphical presentations which may be of greatest convenience for understanding experimental implications. From the polaron form (2.9) [see also Fig. 2(b)] we can expect that our results should reduce to the pure dimerized limit (with appropriate level occupations

at the top and bottom of bands) as $\omega_0 \to \Delta_0$ and to an infinitely separated $K\bar{K}$ pair (i.e., twice the kink results) as $\omega_0 \to 0$. Explicit evaluations of the results described above confirm that these limits are indeed satisfied. We can show the following:

(a) As $\omega_0 \to \Delta_0$, the integrated intensities behave as

$$\int \alpha_P^{(3)}(\omega)d\omega \to 0 ,$$

$$\int \alpha_P^{(2)}d\omega \to \int \alpha_P^{(1)}(\omega)d\omega \to \tfrac{1}{2}A\pi\xi_0/L ,$$

$$\int \alpha_P^{\mathrm{IB}}(\text{off-diag})(\omega)d\omega \to 0 ,$$

$$\int \alpha_P^{\mathrm{IB}}(\text{diag})(\omega)d\omega \to \tfrac{1}{2}A(1-\pi\xi_0/L) .$$

Thus the sum rule (3.3) is satisfied. Notice that although the distribution of weights among transitions depends on the occupation of localized levels, the *total* weight involving localized levels is independent of this consideration (the wave functions are independent of occupation numbers within our model). This is ncessarily so, in general, in view of the sum rule (3.3), and is demonstrated in Fig. 6 where we show the total integrated weight taken out of interband transitions by the presence of a polaron; the result depends only on ω_0 and not on localized level occupation. The same is trivially true of a kink or any combination of kinks and polarons.

(b) As $\omega_0 \to 0$, the absorption coefficient components behave as

$$\int \alpha_P^{(1)}(\omega)d\omega \to \pi A\frac{\xi_0}{L}\frac{\omega_0}{\Delta_0}\ln\frac{\omega_0}{\Delta_0} \to 0 ,$$

$$\alpha_P^{(2)}(\omega) \to \alpha_P^{(3)}(\omega) \to \tfrac{1}{2}A\pi^2\frac{\xi_0}{L}(\omega^2-\Delta_0^2)^{1/2} \times \mathrm{sech}^2\left[\frac{\pi}{2\Delta_0}(\omega^2-\Delta_0^2)^{1/2}\right]$$

[i.e., twice the single kink result (3.4)], and

$$\int \alpha_P^{\mathrm{IB}}(\text{diag})(\omega)d\omega \sim A\frac{\xi_0}{L}\ln\left[\left[\frac{2\Delta_0}{\omega_0}\right]^4\right] .$$

$[\alpha_P^{\mathrm{IB}}(\omega)]$ (diag + off-diag) will be discussed below.

One very striking feature of our results is the difference between $\alpha_P^{(2)}(\omega)$ and $\alpha_P^{(3)}(\omega)$ (see Fig. 7) near their respective thresholds; from (3.9), $\alpha_P^{(2)}$ has a square-root singularity

$$\alpha_P^{(2)}(\omega) \underset{\omega\to\Delta_0-\omega_0}{\sim} A\frac{\xi_0}{L}\frac{\pi^2}{2}\frac{1}{(K_0\xi_0)^3}\left[1-\frac{\omega_0}{\Delta_0}\right] \times \frac{1}{[(\omega+\omega_0)^2-\Delta_0]^{1/2}} \qquad (4.1)$$

of the same form as for the kink case (3.4); however, from (3.10), $\alpha_P^{(3)}$ tends to zero at threshold according to

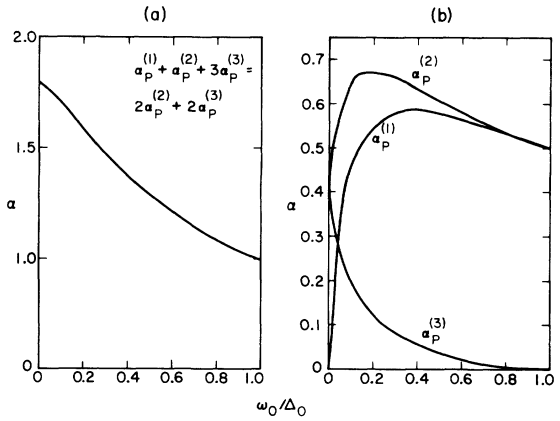

FIG. 6. (a) Total integrated weight (in units of $\pi\xi_0/L$) of transitions involving localized levels as a function of ω_0. Note that this weight is independent of level occupation. (b) Integrated weights (in units of $\pi\xi_0/L$) of single transitions involving localized levels as a function of ω_0. For notation see Fig. 5(c). Note the order-of-magnitude difference between $\alpha_P^{(2)}$ and $\alpha_P^{(3)}$ for $\omega_0 \gtrsim 0.2\Delta$.

$$\alpha_P^{(3)}\omega \underset{\omega\to\Delta_0+\omega_0}{\sim} A\frac{\xi_0}{L}\frac{\pi^2}{8}\left[1-\frac{2y_0}{\xi_0}\right]^2\frac{1}{(K_0\xi_0)^3}\frac{(\Delta_0+\omega_0)}{\Delta_0^3} \times[(\omega-\omega_0)^2-\Delta_0^2]^{+1/2} . \qquad (4.2)$$

These differences appear surprising if we view the localized levels at $\pm\omega_0$ too naively as bonding and antibonding levels due to overlap of two midgap kink states. In fact, the charge-conjugation symmetry in our model implies (see Appendix) $f_{\pm}^{(-)} = \pm f_{\pm}^{(+)}$, which in turn means that the matrix elements for transitions from, for example, the valence band to the $(-\omega_0)$ and $(+\omega_0)$ localized levels differ as a sum or difference of the *same* f products in (3.2).[35] This means that we change from the real part to the imaginary part of a complex quantity for the two types of transition and leads to the different threshold behaviors (4.1) and (4.2). We can notice also the very different intensities implicit in (4.1) and (4.2) for $\alpha_P^{(2)}(\omega)$ and $\alpha_P^{(3)}(\omega)$; for most values of ω_0 the intensity in valence band to $(+\omega_0)$ or $(-\omega_0)$ to conduction-band transitions is significantly weaker than the other transitions involving localized levels. We have shown all the integrated intensities as a function of ω_0 in Fig. 6(b). It will be seen, for example, that for $\omega_0/\Delta_0 \sim 1/\sqrt{2}$ [appropriate to *trans*-$(CH)_x$; see Sec. II], the overwhelmingly predominant transitions are $\alpha_P^{(1)}$ and $\alpha_P^{(2)}$. Furthermore, the intensity in transitions between the localized levels $\alpha_P^{(1)}$ is roughly half the total; since we can also expect this absorption to be a very narrow

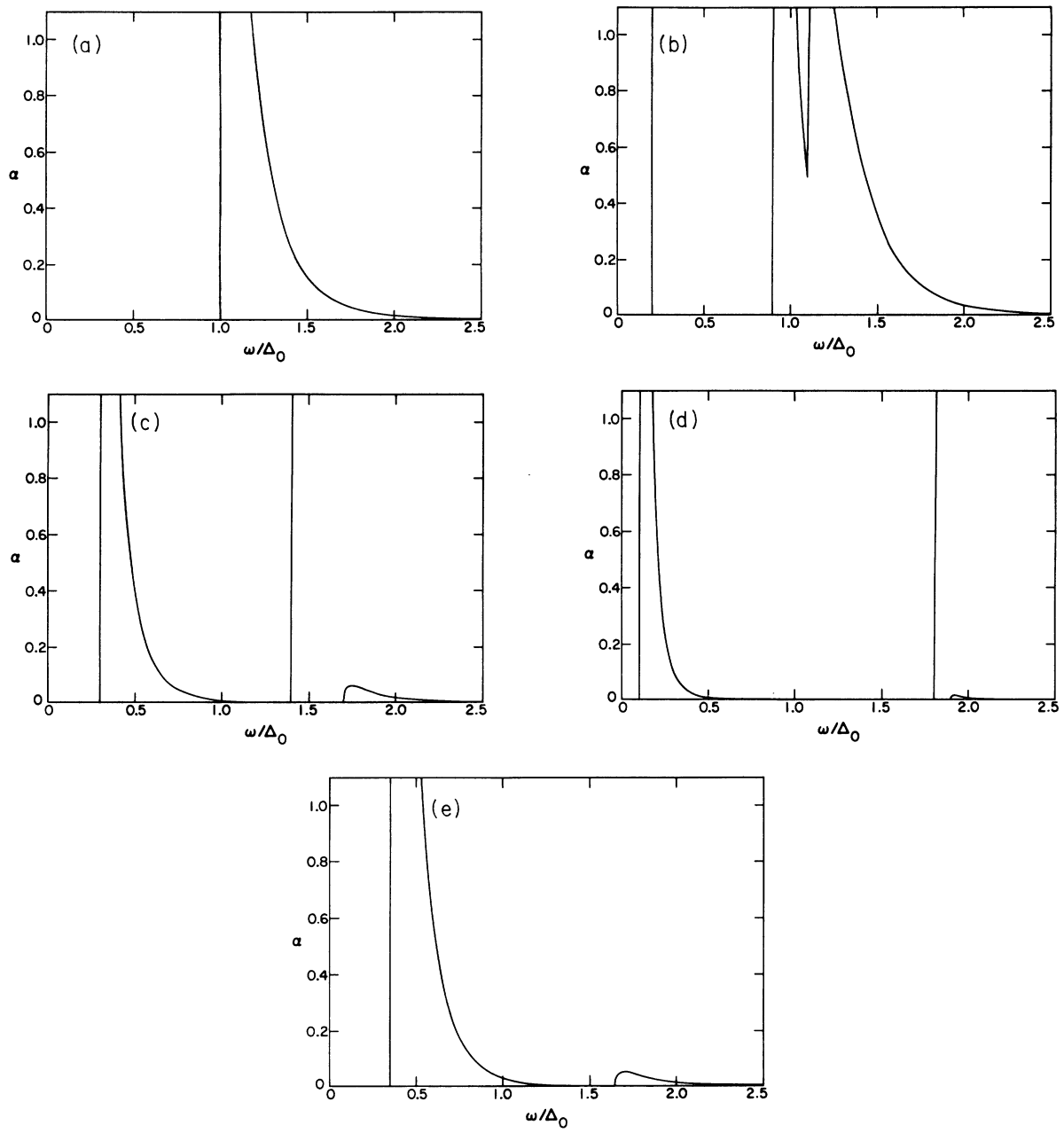

FIG. 7. Optical-absorption spectrum below the gap $\omega=2\Delta_0$, without broadening: (a) single kink; (b) single electron polaron ($n_+=1, n_-=2$) with $\omega_0=0.1\Delta_0$; (c) single electron polaron with $\omega_0=\Delta_0/\sqrt{2}$ [*trans*-$(CH)_x$]; (d) single electron polaron with $\omega_0=0.9\Delta_0$; (e) single bipolaron ($n_+=n_-=0$ or 2) with $\omega_0=0.65\Delta_0$.

feature in frequency (see also Fig. 7), it may be a useful experimental label (see also Sec. V). As we noted above, $\int \alpha_P^{(3)}(\omega)d\omega$ grows to $\int \alpha_P^{(2)}(\omega)d\omega$, as $\omega_0 \to 0$ (i.e., $y_0 \to \infty$; see Fig. 6), but the singularity structures (4.1) and (4.2) are maintained for all ω_0.

In Fig. 7(a) we illustrate absorption spectra predicted from a kink and in Figs. 7(b)–7(d) from an electron (or hole) polaron with three representative choices of ω_0. Figure 7(e) shows the same information for a choice of electron (or hole) bipolaron. Figure 8 shows three examples from Fig. 7 in which a Gaussian function has been convoluted with the theoretical results to represent reasonable broadening.

Finally, in Fig. 9 we show results of numerical integration for the interband optical absorption in the

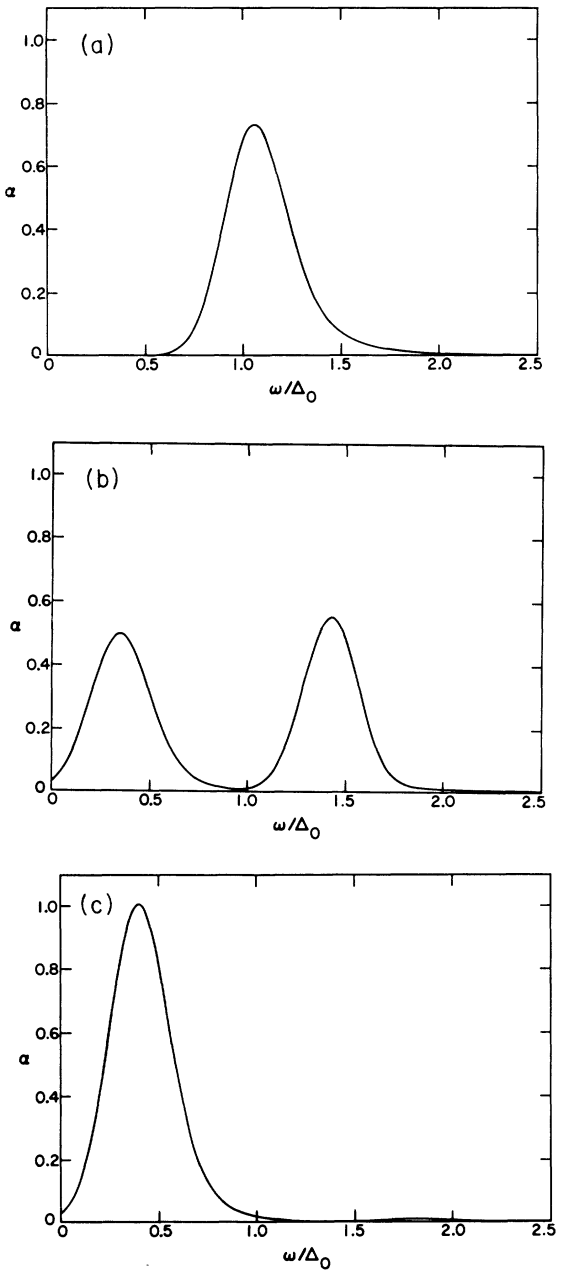

FIG. 8. Optical-absorption spectrum (in arbitrary units) below the gap $\omega=2\Delta_0$ with a Gaussian broadening of $\sigma=0.14\Delta_0$: (a) single kink; (b) single electron polaron with $\omega_0=\Delta_0/\sqrt{2}$ [*trans*-$(CH)_x$]; (c) single bipolaron with $\omega_0=0.65\Delta_0$.

presence of polarons; recall that this depends only on ω_0 and the number of polarons. We have assumed a low concentration c of polarons ($c=0.02$), such that our one-polaron results can be taken to be additive, and plotted

$$\alpha_P^{\mathrm{IB}}(\omega)\equiv\alpha_D(\omega)[1-c\beta(\omega)]\ . \tag{4.3}$$

A striking feature of $\beta(\omega)$ for *kinks*, Eq. (3.6a), is that it is essentially independent of frequency above the threshold $\omega=2\Delta_0$. Interestingly, for polarons there is also a uniform asymptotic structure to $\beta(\omega)$ [see Fig. 9(a)] which tends to zero for $\omega_0\to\Delta_0$. In addition, there is a growing absorption localized to $\omega\gtrsim 2\Delta_0$, as $\omega_0\to\Delta_0$, which approaches a δ function at $\omega_0=\Delta_0$. Recall that the integrated intensity $\int\alpha_D(\omega)\beta(\omega)d\omega$ also decreases with increasing ω_0 [Fig. 6(a)]. In the opposite limit $\omega_0\to 0$, $\beta(\omega)$ is shown in Fig. 9(b): We can see the development of a sharp peak at $\omega=2\Delta_0$ together with a minimum right after this peak. This is due to the fact that in this limit the polaron profile tends to a widely separated pair of kink and antikink whose width becomes smaller and smaller. Thus the chain is mainly purely dimerized giving rise to the peak at $\omega=2\Delta_0$. Only for very large frequencies $\omega\gg 20\Delta_0$ does $\beta(\omega)$ reach its asymptotic value of 4, which is twice the single kink result. This crossover from polaron (bound kink-antikink pair) to widely separated kink-antikink behavior appears when the distance between the kinks ($2y_0$) becomes greater than the width ($2/K_0$) of the individual kink: $2y_0=4/K_0$, which gives ω_0(crossover) $\simeq 0.26\Delta_0$. This is in complete agreement with our results [see Figs. 9(a) and 9(b)]. Figure 9(c) shows a result for $\alpha_P^{\mathrm{IB}}(\omega)$ without broadening and Fig. 9(d) includes the same Gaussian broadening used in Fig. 8.

V. DISCUSSION

In the previous sections we have described in detail kink, polaron, and bipolaron excitations as they appear in certain continuum electron-phonon models of *trans*- and *cis*-polyacetylene (Sec. II). These models have the great advantage of admitting analytic solutions because of partial soliton (reflectionless-potential) properties. In Sec. III we took advantage of these attractive features to evaluate the optical-absorption coefficients from isolated kinks and polarons. The kink result duplicates existing calculations,[7,18,20] but the polaron results are new and contain some surprises (Sec. IV). As explained in Sec. II, the presence of a single kink (or antikink) induces a single localized electronic state at the *middle* ($\epsilon=0$; the Fermi energy) of a semiconductor gap ($-\Delta_0,+\Delta_0$), with density of states taken from the conduction and valence bands. A polaron induces *two* localized gap states, symmetrically disposed about midgap at $\epsilon=\pm\omega_0$. The dimerized lattice distortion corresponding to the polaron (Sec. II) has the form of a bound kink-antikink pair defined by just one parameter (K_0 or y_0 in Sec. II); $K\bar{K}$ separation and shape are specifically related. This parameter is itself related to ω_0. For *trans*-$(CH)_x$

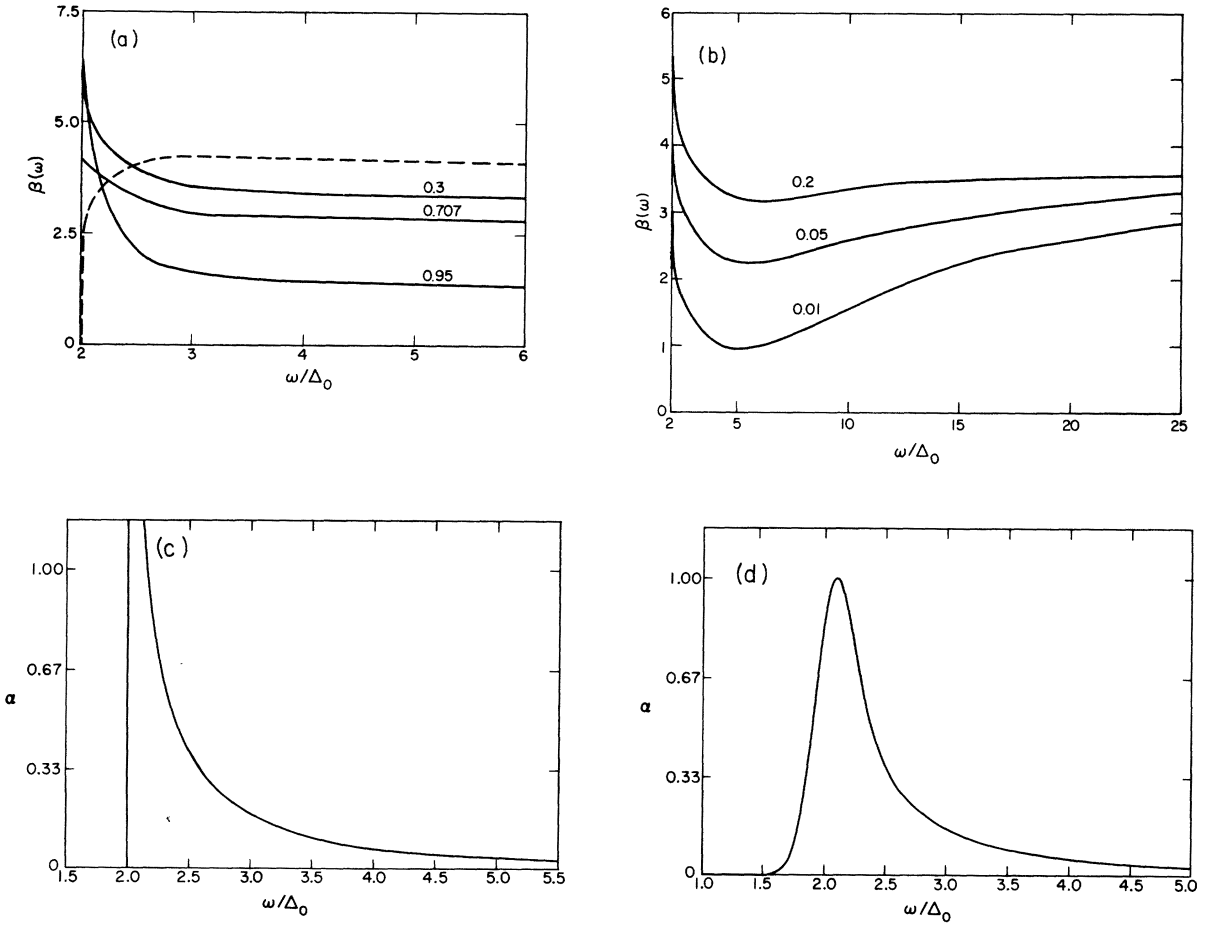

FIG. 9. (a) Spectral weight $\beta(\omega)$ (see Sec. IV) taken out of the interband transition in the presence of a single polaron for three different values of ω_0 (solid lines). The dashed line is twice the result for a single kink. (b) $\beta(\omega)$ for three different values of ω_0/Δ_0: 0.01, 0.05, and 0.2. Note that for $\omega_0 \to 0$ (kink limit), $\beta(\omega)$ reaches its asymptotic value $\{[\beta(\omega) \gg 2\Delta_0] = 4\}$ only for very large values of ω ($\omega > 50\Delta_0$). (c) Optical-absorption spectrum (in arbitrary units) of the interband transition in presence of a single polaron without broadening. (d) The same as (c) with a Gaussian broadening of $\sigma = 0.14\Delta_0$.

only one value of ω_0 ($1/\sqrt{2}$) associated with two localized state occupations (corresponding to a singly occupied electron or hole polaron) is stable against decay to either the ground state ($\omega_0 = \Delta_0$) or widely separated $K\bar{K}$ ($\omega_0 \to 0$). In *cis*-$(CH)_x$, however, free kinks are *not* allowed because of the absence of degenerate ground states. Further, polarons are stable whether singly occupied or doubly occupied (electron-electron, hole-hole, or electron-hole bipolarons). The relevant value of ω_0 is determined (from Fig. 4) by a combination of the relative level ($\epsilon = \pm\omega_0$) occupations and a "confinement" parameter (measuring the extent of degeneracy breaking; Fig. 3). In turn the optical-absorption spectra from a polaron is determined only by the values of ω_0 and the relative level occupation: Our model is remarkable in that the absorption coefficients have the *same* functional form for all ω_0. As for a kink, the optical absorption from a polaron explicitly satisfies a sum rule, Eq. (3.3), which is known to hold in some generality.[18,19] The distribution of absorption in frequency has more structure, however, because of the additional localized electronic levels. For a kink there is one absorption peak below the interband threshold with a square-root divergence at midgap ($\omega = \Delta_0$). For a singly occupied polaron there are three peaks below the interband threshold due to transitions between the localized levels and between these and the extended conduction- or valence-band states. The bipolaron precludes transitions between the localized levels, so that there are only two peaks below interband threshold. [How-

ever, as for a kink, the integrated intensity from structures in the gap is independent of localized state occupation; Fig. 6(a).] The number of independent transitions is reduced by the "charge-conjugation" (particle-hole) symmetry (see Appendix) of our system. This same symmetry is responsible (see Appendix) for a striking asymmetry in the absorptions from transitions between localized and extended states: Namely (see Fig. 7), the lower-frequency structure has a square-root divergence at its threshold ($\omega=\Delta_0-\omega_0$), whereas the higher-frequency structure tends to zero at its threshold ($\omega=\Delta_0+\omega_0$). The integrated intensities in these two components are also very asymmetric, except for widely separated $K\bar{K}$ ($y_0\to\infty,\omega_0\to 0$), where the free kink result is recovered.

It is important to emphasize that the basic features above are a result of a general symmetry property rather than more specific details of the models (2.2) and (2.16). Other models may lack the same elegant analytic accessibility but can retain the essential absorption structure.

A brief discussion of experimental consequences of, and observation of, polarons in conjugated polymers is in order. On energy grounds we expect (Sec. II) that single-electron or hole doping in *trans*-$(CH)_x$ will initially induce polarons which, when more than one polaron exists on a single chain, will combine to form "free" kinks and antikinks.[14] This view is supported by the quantified hysteresis observed in recent electrochemical doping and compensation measurements[14] ("voltage spectroscopy"). On the other hand, at light doping levels, and especially in view of finite chain segments and uncertain interaction dynamics for the polarons, we can anticipate that *singly* occupied polarons will occur (in addition to kinks and antikinks) in *trans*-$(CH)_x$. All three types of transitions in Fig. 7 would contribute in this case, but the weights indicated in Fig. 6 imply (with $\omega_0\simeq\Delta_0/\sqrt{2}$) *two* significant (approximately equal weight) absorption peaks (in addition to the kink midgap absorption) around $\omega\simeq\Delta_0-\omega_0$ and $2\omega_0$ with the latter being *narrower*. It is believed[14] that this narrow peak has indeed been observed in optical-absorption experiments on electrochemically doped *trans*-$(CH)_x$ films. Further evidence for a polaron interpretation would be the observation of low-frequency structure ($\omega\simeq\Delta_0-\omega_0$) *correlated* with the high-frequency one. Unfortunately, the relevant low-frequency regime is in the infrared (ir) where many structures are expected and even more observed. A promising complement to this search for polarons in *trans*-$(CH)_x$ is optical-absorption evidence[17] for *hole bipolarons* in as-formed and doped *cis*-$(CH)_x$. A possible interpretation here is that, as in *trans*-$(CH)_x$, a small concentration of positively charged defects ($\sim$200 ppm) is formed during the synthesis of *cis*-$(CH)_x$. As explained in Sec. II, these must appear as polarons in the cis isomer, and on energy grounds bipolarons are preferred; again the actual formation kinetics requires a deeper understanding of polaron collision and hopping mechanisms. In this case the narrow absorption structure from transitions between localized levels would be prohibited, and predominant absorption would be in a broad peak at $\omega\approx\omega_0-\Delta_0$. Absorption data has been shown to be consistent with a bipolaron interpretation with, in the model (2.16), $\gamma\approx 0.67$ (implying $\omega_0/\tilde{\Delta}_0\approx 0.67$ from Fig. 4) and $\Delta_e\approx\Delta_i^0\approx 1$ eV.[17] Under doping, there is evidence that cis-trans isomerization occurs inhomogeneously[36] in the dopant regions (distinct from the as-formed defect regions); then kinks and antikinks should be preferentially induced in these trans regions, with the polarons in the cis regions substantially unaffected. Optical-absorption data under doping and compensation of *cis*-$(CH)_x$ (Refs. 7, 8, and 14) are again consistent with this interpretation, although once more definitive evidence (e.g., charge and spin assignments) will be required. Clearly, conjugated polymers more optimal for polarons and bipolarons need to be studied systematically. Several potential materials exist where *kink*-bearing environments (i.e., *degenerate* phases) do not exist and are not induced by doping. Polyparaphenylenes seem especially worthy of detailed study in view of their high conductivity under light doping and existing numerical modeling[11] of polarons (and bipolarons).

Although we have concentrated on optical absorption, it should be clear that polaron excitations will need to be folded into the interpretation of a range of (existing and forthcoming) experimental data in conjugated polymers: ESR, ir, photoconductivity and photoluminescence, transport, doping, etc. It is worthwhile emphasizing that kink-lattice "melting" theories[22] of the insulator-metal transition observed in $(CH)_x$ generalize very obviously to polaron (or bipolaron) lattice theories appropriate to a wider range of polymers.[37]

Having stressed the optical absorption from polarons within the model described in Sec. II, we need to appreciate potentially important corrections to that model. We have not included any description of *dynamics*, which is an uncertain area both for kinks *and* polarons in the SSH model (2.1). Internal (shape) vibrations coupled to translations can be expected and the extended,[6,38] strongly nonlinear, quasisoliton character of the excitations could well lead to nontrivial interactions between excitations; these interactions are of considerable importance in understanding, for example, *time scales* for decay channels dictated by equilibrium energy considera-

tions [e.g., polaron+polaron$\rightarrow K\bar{K}$ in *trans*-$(CH)_x$ or $K\bar{K}$ recombination after photoabsorption in *cis*-$(CH)_x$]. Likewise, polaron transport in the SSH model (diffusion along chains and hopping between chains) is a quite open area, as is the description of a polaron band or shakeoff phonon structure. With the use of a conventional adiabatic technique one can estimate the kink mass M_K in the SSH model.[1] The same adiabatic estimate (neglecting all internal modes) for the polarons yields a mass M_P given (in the continuum limit) by[34]

$$M_P(\omega_0)=2M_K(K_0\xi_0)^3 \times\left[1-3\frac{(\omega_0/\Delta_0)^2}{K_0^2\xi_0^2}\left[2\frac{y_0}{\xi_0}-1\right]\right], \quad (5.1)$$

which we have plotted in Fig. 10. Realistic parameters for *trans*-$(CH)_x$ suggest $M_P/M_e \lesssim 1$, and for the bipolaron in *cis*-$(CH)_x$, $M_P/M_e \simeq 3$, where M_e is an electron mass. These light masses highlight the likely importance of *quantum* corrections. Nakahara and Maki[38] have suggested that quantum renormalization of the adiabatic limit (as used in Secs. II–IV) can be pronounced even for the kink ($M_K \gtrsim 3M_e$) but is not sufficient to destabilize the polaron. In fact, we feel that quantum fluctuations will be strongly suppressed even by weak interchain coupling. Nevertheless, *relative* effects on E_K, E_P, and Δ_0 need to be considered. Effects of electron-electron interactions are also very rich. It has been argued[1,39] that these effects are weak in $(CH)_x$, at least for excitations about an effective ground state. The *relative* differences among varieties of kinks and polarons are interesting. More importantly, *qualitatively* new phenomena can be introduced by e-e interactions, if not in $(CH)_x$, certainly in other conjugated polymers: for example, excitons [or more generally exciton-polarons; c.f. the electron-hole bipolaron ($n_+=n_-=1$)], recombination barriers, and "negative U" states [sometimes called bipolarons but referring to confinement in the presence of e-e interactions rather than the energy nondegeneracy of model (2.16)].[40] The strong exciton observed[41] in the band gap of certain polydiacetylenes may serve as an example. The roles of impurities, crosslinks, chain defects, etc., as pinning or scattering centers are also unassessed here.[42] A variety of (inhomogeneous) line-broadening effects can be expected; we have included an example of phenomenological broadening in the absorption spectra shown in Fig. 8, which is representative of experimentally observed spectra. The smearing of the interband optical-absorption edge, for example, is outside the range of our present calculations. This could be introduced by including, for example, a finite concentration of inhomogeneously distributed (kink or polaron) defects, interchain coupling, or e-e interactions. Finally, we have neglected any relaxation channels for excited electronic states achieved through optical transitions. A key point here is the validity of our adiabatic assumptions which determine relaxation time scales and the nature of sideband frequency structures.[43]

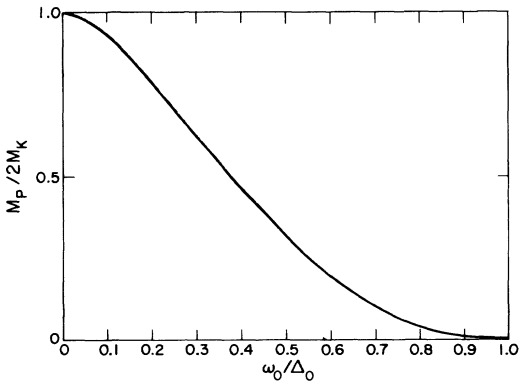

FIG. 10. Mass of a polaron in units of twice the kink mass as a function of ω_0. (Calculated in an adiabatic approximation—see Ref. 34.)

Some of the effects described above, especially if they destroy the important symmetries of the basic Hamiltonian (2.1), can remove the relationships (weights, locations) among the three absorption components in the gap described in Secs. III and IV. Nevertheless, the results outlined are sufficiently rich and novel to be a suggestive first approximation to the optical absorption in $(CH)_x$.

In conclusion, we wish to reiterate the reason for our preoccupation with polarons (and excitons) in conjugated polymers. *Trans*-$(CH)_x$ is unusual in possessing *degenerate* ground states and therefore "free" kinks. A unique ground state with additional metastable conformations is the much more typical case (e.g., polyparaphenylenes, polypyrroles, polydiacetylenes). Experimental observations[44] show that these circumstances do not necessarily preclude large conductivity increases under light doping, but theoretically they do exclude free kink solitons. Thus polarons and excitons (and combinations of these), although more familiar than kinks (with their unusual spin-charge assignments), are *more generic;* they do not even require a double-well structure at all. In the developing effort to understand a wide class of conducting conjugated polymers, the role of polarons is likely to be central. Furthermore, the theory of polarons and excitons in quasi-one-dimensional systems (i.e., a *mixed* diffusive-hopping environment) is incomplete, challenging, and, in view of new materials interests, wholly relevant. As we have seen, the model considered in this paper has certain special properties relevant to the structure of

$(CH)_x$; some generalizations are necessary to encompass the full spectrum of conducting polymers, but the concern with polarons and excitons in anisotropic environments is quite general.

ACKNOWLEDGMENTS

It is a pleasure to thank Baruch Horovitz, Steve Kivelson, and Bob Schrieffer for a number of valuable conversations concerning the theoretical aspects of our calculations, and Art Epstein and Shahab Etemad for sharing their insights into the experimental possibilities for detecting polarons in these quasi-one-dimensional polymers. Two of us (K.F. and A.R.B.) wish to thank the Institute for Theoretical Physics at Santa Barbara for its hospitality during the early stages of this work. This work has been supported by the U. S. Department of Energy.

APPENDIX

In this Appendix we collect and make explicit a number of technical details needed in the calculations described in the text. We begin by discussing the consequences of the "charge-conjugation" or "electron-hole" symmetry of the continuum electron-phonon-coupled equations (2.3). This symmetry is that, given a solution U_n, V_n with energy ϵ_n, one can find a solution U_{-n}, V_{-n} with energy $-\epsilon_n$ simply by the replacement

$$U_{-n}=iV_n\ , \qquad V_{-n}=-iU_n\ . \tag{A1}$$

The proof is by straightforward algebra.

In terms of the functions $f_\pm \equiv U \pm iV$ introduced in the text, this symmetry is even simpler and reads

$$f_\pm^{(-n)}=\pm f_\pm^{(+n)}\ . \tag{A2}$$

Clearly, this symmetry applies to both continuum and discrete states.

Apart from this simplification of the particle-hole symmetry, $f_\pm$ are useful because, from the Dirac equations (2.3), they satisfy more familiar Schrödinger equations. From (2.3) it follows directly that

$$-v_F^2\frac{d^2}{dy^2}f_\pm^{(n)}+\left[\Delta^2\mp v_F\frac{d\Delta}{dy}\right]f_\pm^{(n)}=\epsilon_n^2 f_\pm^{(n)}\ , \tag{A3}$$

so that the Schrödinger potentials relevant to $f_\pm$ are

$$V_\pm^{\rm Sch}=\Delta^2\mp v_F\frac{d\Delta}{dy}\ . \tag{A4}$$

In the case of the polaron, using the explicit form of $\Delta_P(x)$ given in (2.9a), (A4) becomes (after some algebra)

$$V_\pm^{\rm Sch}=\Delta_0^2-2K_0^2v_F^2\,\mathrm{sech}^2[K_0(y\mp y_0)]\ . \tag{A5}$$

Considering the factor v_F associated with the y scale of (A5), we recognize $V_\pm^{\rm Sch}$ as the well-known reflectionless Schrödinger potentials having precisely one bound state.[45] Thus, in a sense, the $f_\pm$ reveal in a more familiar way the solitonlike structure underlying the polaron solution in $(CH)_x$. At a more technical level, (A5) shows directly that for the polaron the $f_\pm$ involve only functions of $(y\mp y_0)$, respectively, and hence motivates the simple structures of the explicit forms of the bound state and continuum $f_\pm$.

From the general discussion of the optical absorption in the text we know that the relevant matrix element for a transition between an initial state k and a final state k' can be written

$$M_{k'k}=\tfrac{1}{2}\int dy[f_+^*(k')f_-(k)+f_-^*(k')f_+(k)]\ . \tag{A6}$$

For the polaron, there are six classes of transitions with the six matrix elements: $M^P_{+0,-0}$, $M^P_{c,+0}$, $M^P_{+0,v}$, $M^P_{-0,v}$, and $M^P_{c,+v}$. Here, we have used the notation c (v) for the conduction- (valence-) band state and $+0$ (-0) for the positive- (negative-) energy band state.

With the use of the "particle-hole" symmetry equation (A2), it is straightforward to establish relations among certain transitions. Specifically,

$$\begin{aligned}M^P_{c,+0}&=\tfrac{1}{2}\int(f_+^{c*}f_-^{+0}+f_-^{c*}f_+^{+0})dy\\&=\tfrac{1}{2}\int(-f_+^{v*}f_-^{-0}-f_-^{v*}f_+^{-0})dy\\&=-\left[\tfrac{1}{2}\int(f_-^{v*}f_+^{-0}+f_+^{-0*}f_-^{v})dy\right]^*\\&=-M^{P*}_{-0,v}\end{aligned} \tag{A7a}$$

and

$$\begin{aligned}M^P_{c,-0}&=\tfrac{1}{2}\int(f_+^{c*}f_-^{-0}+f_-^{c*}f_+^{-0})dy\\&=\tfrac{1}{2}\int(-f_+^{v*}f_-^{+0}-f_-^{v*}f_+^{+0})dy\\&=-\left[\tfrac{1}{2}\int(f_-^{+0*}f_+^{v}+f_+^{+0*}f_-^{v})dy\right]^*\\&=-M^{P*}_{+0,v}\ .\end{aligned} \tag{A7b}$$

Since only $|M|^2$ enters in α, we see that (A7a) implies $\alpha^P_{c,0}=\alpha^P_{-0,v}\equiv\alpha_P^{(3)}$ and (A7b) implies $\alpha^P_{c,-0}=\alpha^P_{0,v}\equiv\alpha_P^{(2)}$ (see Fig. 5), where we have introduced the simplified notation we use in the text. Thus there are only four independent matrix elements to evaluate. Let us first consider the three transitions involving the localized levels.

1. $M^P_{+0,-0}$

From (A8) we have

$$M^P_{+0,-0}=\tfrac{1}{2}\int (f_+^{+0*}f_-^{-0}+f_-^{+0*}f_+^{-0})dy \ . \quad \text{(A8)}$$

Using the explicit forms of $f_\pm$ from Eqs. (2.12) and (A2), we find directly

$$M^P_{0,-0}=\frac{16i}{2}\frac{K_0}{16}\int_{-\infty}^{\infty} dy\,\mathrm{sech}[K_0(y+y_0)] \times\mathrm{sech}[K_0(y-y_0)] \ . \quad \text{(A9)}$$

The integral in (A9) is the $k\to 0$ limit of the Fourier transform

$$I_1\equiv\int_{-\infty}^{\infty} dy\,e^{iky}\mathrm{sech}[K_0(y+y_0)]\times\mathrm{sech}[K_0(y-y_0)] =2\int_{-\infty}^{\infty}\frac{dy\,e^{iky}}{\cosh(2K_0y)+\cosh(2K_0y_0)} \ , \quad \text{(A10)}$$

which can be obtained either from the tables or directly by contour integration along the contour shown in Fig. 11. The result is, recalling $\sinh 2K_0y_0=K_0v_F/\omega_0$,

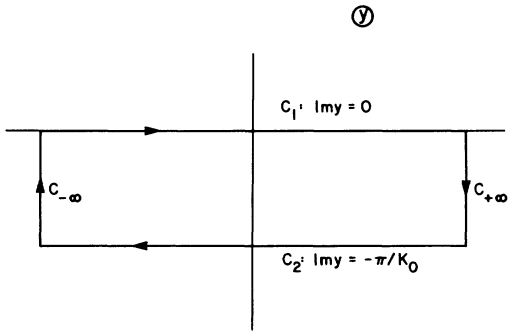

FIG. 11. Contour of integration in the complex y plane (see Appendix).

$$I_1=\frac{4\omega_0y_0}{K_0v_F} \ , \quad \text{(A11)}$$

which leads to the expression in the text

$$M^P_{+0,-0}=2i\omega_0y_0/v_F \quad \text{(A12)}$$

for $\alpha^P_{+0,-0}\equiv\alpha_P^{(1)}$.

2. $M^P_{c,+0}$

From (A6) we have

$$M^P_{c,+0}=\tfrac{1}{2}\int dy(f^{c*}_{P+}f^{+0}_{-}+f^{c*}_{P-}f^{+0}_{+}) =4iN_P(k)N_P^0\int dy\,e^{-iky}\left[\gamma(k)\left[\frac{k}{K_0}-i\tanh[K_0(y-y_0)]\right]\mathrm{sech}[K_0(y+y_0)] +\gamma^*(k)\left[\frac{k}{K_0}-i\tanh[K_0(y+y_0)]\right]\mathrm{sech}[K_0(y-y_0)]\right] \ , \quad \text{(A13)}$$

where in the second equality we have used the explicit form of the $f_\pm$ from Eqs. (2.10).

Again the integrals can be evaluated using the contour shown in Fig. 11. We find

$$\int dy\,e^{-iky}\mathrm{sech}[K_0(y+y_0)]=\left[\int dy\,e^{-iky}\mathrm{sech}[K_0(y-y_0)]\right]^*=e^{+iky_0}\frac{\pi}{K_0}\mathrm{sech}\left[\frac{\pi k}{2K_0}\right] \quad \text{(A14a)}$$

and

$$\int dy\,e^{-iky}\tanh[K_0(y-y_0)]\mathrm{sech}[K_0(y+y_0)]=-\left[\int dy\,e^{-iky}\tanh[K_0(y+y_0)]\mathrm{sech}[K_0(y-y_0)]\right]^* =\frac{1}{K_0\xi_0}\frac{\pi}{K_0}\mathrm{sech}\left[\frac{\pi k}{2K_0}\frac{\omega_0}{\Delta_0}e^{-iky_0}-e^{+iky_0}\right] \ . \quad \text{(A14b)}$$

To derive these expressions we have used the results $\tanh 2K_0y_0=K_0\xi_0$ and $\mathrm{sech}2K_0y_0=\omega_0/\Delta_0$ [see Eq. (2.9b)]. Further, the correctness of the relations among the integrals shown in (A14) can be verified directly by a change of variables. Using these relations we see that

$$\beta(k)\equiv\int dy\left[\frac{k}{K_0}-i\tanh[K_0(y-y_0)]\right]\mathrm{sech}[K_0(y+y_0)]e^{-iky}$$
$$=\left[\int dy\left[\frac{k}{K_0}-i\tanh[K_0(y+y_0)]\right]\mathrm{sech}[K_0(y-y_0)]e^{-iky}\right]^* \tag{A15}$$

and thus that

$$M^P_{c,+0}=4iN_P(k)N^0_P[\gamma(k)\beta(k)+\gamma^*(k)\beta^*(k)]\ , \tag{A16}$$

where from (A14) and (A15)

$$\beta(k)=\frac{1}{K_0v_F}\frac{\pi}{K_0}\mathrm{sech}\left[\frac{\pi k}{2K_0}\right]\{[kv_F+i(\Delta_0-\omega_0)]\cos(ky_0)+[ikv_F-(\Delta_0+\omega_0)]\sin(ky_0)\}\ . \tag{A17}$$

Using (A17) and the expression for $\gamma(k)$ from (2.6b), we obtain finally the result quoted in the text,

$$M^P_{c,+0}=4iN_P(k)N^0_P\frac{\pi}{K_0}\mathrm{sech}\left[\frac{\pi k}{2K_0}\right]\frac{\epsilon_k-\omega_0}{\Delta_0}\left[\sin(ky_0)+\frac{kv_F}{\epsilon_k-\Delta_0}\cos(ky_0)\right]\ . \tag{A18}$$

3. $M^P_{c,-0}$

From (A8) we have

$$M^P_{c,-0}=\tfrac{1}{2}\int dx(f^{c^*}_{P+}f^{-0}_{-}+f^{c^*}_{P-}f^{-0}_{+}) \tag{A19a}$$
$$=4iN_P(k)N^0_P\int dy\,e^{-iky}\left[-\gamma(k)\left[\frac{k}{K_0}-i\tanh[K_0(y-y_0)]\right]\mathrm{sech}[K_0(y+y_0)]\right.$$
$$\left.+\gamma^*(k)\left[\frac{k}{K_0}-i\tanh[K_0(y+y_0)]\right]\mathrm{sech}[K_0(y-y_0)]\right]\ . \tag{A19b}$$

From the previous discussion and definitions we see that this can be written as

$$M^P_{c,-0}=4iN_P(k)N^0_P[-\gamma(k)\beta(k)+\gamma^*(k)\beta^*(k)]\ , \tag{A20a}$$

which, after some algebra, leads to the explicit result used in the text

$$M^P_{c,-0}=4iN_P(k)N^0_P\frac{\pi}{K_0}\mathrm{sech}\left[\frac{\pi k}{2K_0}\right]\frac{\epsilon_k+\omega_0}{\Delta_0}\left[\frac{kv_F}{\epsilon_k-\Delta_0}\sin(ky_0)-\cos(ky_0)\right]\ . \tag{A20b}$$

We turn next to the matrix element—$M^P_{c,v}$—which determines the interband transition in the presence of the polaron. From (A8) we have

$$M^P_{c,v}=\tfrac{1}{2}\int dx(f^{c^*}_{P+}f^{v}_{P-}+f^{c^*}_{P-}f^{v}_{P+}) \tag{A21a}$$
$$=-4iN_P(k)N_P(k')\int dy\,e^{-i(k'-k)y}\left[\gamma(k')\gamma(k)\left[\frac{k'}{K_0}-it_-\right]\left[\frac{k}{K_0}+it_+\right]\right.$$
$$\left.+\gamma^*(k')\gamma^*(k)\left[\frac{k'}{K_0}-it_+\right]\left[\frac{k}{K_0}+it_-\right]\right]\ , \tag{A21b}$$

where $k'(k)$ is the wave vector of the state in the conduction (valence) band and we have used the abbreviations $t_\pm\equiv\tanh[K_0(y\pm y_0)]$. It is convenient to write this as a sum of three terms

$$M^P_{c,v}\equiv M_1+M_2+M_3\ , \tag{A22a}$$

with

$$M_1=-4iN_P(k)N_P(k')\int dy\, e^{-i(k'-k)y}\left[\frac{k'k}{K_0^2}+1\right][\gamma(k')\gamma(k)+\gamma^*(k')\gamma^*(k)]\ , \tag{A22b}$$

$$M_2=-4iN_P(k)N_P(k')\int dy\, e^{-i(k'-k)y}\left[it_+\frac{\gamma(k')\gamma(k)k'-\gamma^*(k')\gamma^*(k)k}{K_0}\right.$$
$$\left.-it_-\frac{\gamma(k')\gamma(k)k-\gamma^*(k')\gamma^*(k)k'}{K_0}\right], \tag{A22c}$$

and

$$M_3=-4iN_P(k)N_P(k')\int dy\, e^{-i(k'-k)y}(t_+t_--1)[\gamma(k')\gamma(k)+\gamma^*(k')\gamma^*(k)]\ . \tag{A22d}$$

The y integration in (A22b) simply gives a δ function; note that $2\pi\delta(k'-k)=L\delta_{k',k}$ is the relation between the continuum and discrete δ functions. For the other integrals we find

$$\int dy\, e^{-i(k'-k)y}\tanh[K_0(y\pm y_0)]=\begin{cases}\pm 2y_0\ , & k=k'\\ \dfrac{-i\pi}{K_0}\dfrac{\exp[\pm i(k'-k)y_0]}{\sinh[(k'-k)\pi/2K_0]}\ , & k'\neq k\end{cases} \tag{A23a}$$

where for $k'\neq k$ the integral is regulated by continuing appropriately into the complex y plane and then integrating by parts, and

$$\int dy\, e^{-i(k'-k)y}\{\tanh[K_0(y+y_0)]\tanh[K_0(y-y_0)]-1\}=-2\pi\frac{1}{K_0\xi_0}\frac{\sin[(k'-k)y_0]}{K_0\sinh[(k'-k)\pi/2K_0]}\ , \tag{A23b}$$

where we have again used the contour in Fig. 11.

Using these results, we obtain for M_1

$$M_1=-4iN_P^2(k)\left[\frac{k^2+K_0^2}{K_0^2}\right]2\,\mathrm{Re}[\gamma^2(k)]L\delta_{k',k}\ . \tag{A24a}$$

Here we have used the δ function to set $k'=k$ in the prefactor. For M_2 we obtain, for $k'\neq k$,

$$M_2=-4iN_P(k)N_P(k')\frac{\pi}{K_0}\frac{1}{\sinh[(k'-k)\pi/2K_0]}\left[\left[\frac{k'-k}{K_0}\right]\{2\mathrm{Re}[\gamma(k)\gamma(k')]\}\cos[(k'-k)y_0]\right.$$
$$\left.-\left[\frac{k'-k}{K_0}\right]\{2\,\mathrm{Im}[\gamma(k)\gamma(k')]\}\sin[(k'-k)y_0]\right], \tag{A24b}$$

whereas for $k'=k$

$$M_2=32iN_P^2(k)\frac{k}{K_0}y_0[\mathrm{Im}\gamma(k)]^2\ . \tag{A24c}$$

Finally, for M_3, we find

$$M_3=16iN_P(k)N_P(k')\mathrm{Re}[\gamma(k)\gamma(k')]$$
$$\times\frac{1}{K_0\xi_0}\frac{\sin[(k'-k)y_0]}{K_0\sinh[(k'-k)\pi/2K_0]}\ .$$

Using the explicit forms for $\gamma(k)$ and $N_P(k)$ we see that the full interband matrix element can be written, after some algebra, as

$$M_{c,v}^P=\left[M_1\delta_{k'k}+\frac{1}{L}M_2\right], \tag{A25}$$

where M_1 and M_2 are independent of L. Explicitly,

$$M_1=i\Delta_0/\epsilon_k \tag{A26a}$$

and for $k\neq k'$, M_2 is given by

$$M_2=i\frac{\pi}{K_0}\frac{K_0v_F}{\sinh[(k'-k)\pi/2K_0]}C_\beta$$
$$\times\left[C_1\{\Delta_0\sin[(k'-k)y_0]\right.$$
$$\left.-\tfrac{1}{2}(k'-k)v_F\cos[(k'-k)y_0]\}\right.$$
$$\left.-C_2\left[\frac{(k+k')}{2}v_F\sin[(k'-k)y_0]\right]\right], \tag{A26b}$$

where

$$C_\beta=\frac{1}{(\epsilon_{k'}\epsilon_k)^{1/2}}\frac{1}{(k'^2v_F^2+K_0^2v_F^2)^{1/2}}\times\frac{1}{(k^2v_F^2+K_0^2v_F^2)^{1/2}}$$

and

$$C_1=\sqrt{(\epsilon_{k'}-\Delta_0)(\epsilon_k-\Delta_0)}-\sqrt{(\epsilon_{k'}+\Delta_0)(\epsilon_k+\Delta_0)}\,,$$

$$C_2=\sqrt{(\epsilon_{k'}-\Delta_0)(\epsilon_k+\Delta_0)}+\sqrt{(\epsilon_{k'}+\Delta_0)(\epsilon_k-\Delta_0)}\,,$$

and for $k=k'$, M_2 is

$$M_2=-4i\frac{(K_0v_F)y_0}{K_0^2v_F^2+k^2v_F^2}\epsilon_k\,. \tag{A26c}$$

From Eqs. (A25) and (A26) we can obtain directly the forms of the squared matrix elements used in Eq. (31).

We turn next to two technical points necessary to obtain the terms of $O(1/L)$ correctly in the interband optical transition. From (A25)—or (3.13)—we see that

$$|M_{c,v}^P|^2=\left[|M_1|^2+\frac{1}{L}(M_1^*M_2+M_1^*M_2)\right]\delta_{k',k}+\frac{1}{L^2}|M_2|^2\,. \tag{A27}$$

The first item in (A27)—$|M_1|^2\delta_{k',k}$—is, as shown by (A26a), clearly $O(1)$, whereas the second is $O(1/L)$. Thus to include all terms of $O(1/L)$ correctly, we must notice that for finite L both the density of states over which we integrate in k space *and* the normalizations of the continuum wave functions have $O(1/L)$ corrections. Both these corrections must be applied to the $|M_1|^2$ terms in (A27).

To motivate the correction to the density of states—often called the "phase-shift correction"—we notice that for discrete k the density of states in the presence of the polaron is determined by

$$kL+\phi_P(k)=2n\pi\,, \tag{A28}$$

with $\phi_P(k)=2\tan^{-1}(K_0/k)$ being the phase shift due to the polaron. Hence from (A28) the density of states for the continuum, dn/dk, is given by

$$\frac{dn}{dk}=\frac{L}{2\pi}\left[1+\frac{1}{L}\frac{d\phi_P(k)}{dk}\right]=\frac{L}{2\pi}\left[1-\frac{1}{L}\frac{2K_0}{K_0^2+k^2}\right]. \tag{A29}$$

This explains the factor used in going from the discrete sum to the continuum integral in (3.1).

The correction in the normalization factors follows straightforwardly from the form of the continuum $f_\pm$ in (2.10). Using (2.10) with the infinite L normalization $N_P(k)$ replaced by a (to be determined) finite L factor $\tilde{N}_P(k)$, we see that the normalization condition

$$1=\tfrac{1}{2}\int_{-L/2}^{L/2}|f_+|^2+|f_-|^2dy \tag{A30}$$

in our standard notation and implies, using $t_\pm^2=1-s_\pm^2$,

$$1=\frac{|\tilde{N}_P|^2}{2}8|\gamma(k)|^2\int_{-L/2}^{L/2}dy\left[\frac{2(k^2+K_0^2)}{K_0^2}-s_+^2-s_-^2\right]$$

$$=4|\tilde{N}_P(k)|^2|\gamma(k)|^2\left[\frac{2(k^2+K_0^2)}{K_0^2}L-\frac{4}{K_0}\right], \tag{A31}$$

where the last equality is valid to within exponential corrections in L. Thus to leading order in $1/L$,

$$|\tilde{N}_P(k)|^2=|N_P(k)|^2\left[1+\frac{2K_0}{K_0^2+k^2}\frac{1}{L}+\cdots\right]. \tag{A32}$$

Since $|M_{c,v}^P|^2$ is proportional to $|\tilde{N}_P(k)|^2|\tilde{N}_P(k')|^2$, the full $(1/L)$ correction due to normalization is twice that shown in (A32).

As a last comment on theoretical absorption from polarons, we note that all the above formulas have been calculated as functions of K_0 and ω_0. In view of our discussion in Sec. II, this means that they apply immediately for polarons in *cis*-$(CH)_x$; one need only use the appropriate values of ω_0 and K_0 determined by Eq. (2.17).

Finally, for clarity and completeness, we derive in our conventions the optical absorption for (1) the dimerized ground state, (2) the localized state associated with a kink, and (3) the interband absorption associated with a kink. For the dimerized case, $\Delta(y)=\Delta_0$, the wave functions $f_\pm^{c,v}$ are given in (2.6b). Thus the interband matrix element for the dimerized case is, substituting (2.6b) into (A6) and using the δ function resulting from the y integration to set $k'=k$,

$$M_{c,v}^D=\tfrac{1}{2}|N_D|^2(-4i)\times 2\,\mathrm{Re}\left[\left[1-\frac{ikv_F}{\epsilon_k-\Delta_0}\right]^2\right]L\delta_{k',k}$$

$$=+(i\Delta_0/\epsilon_k)\delta_{k',k}\,, \tag{A33}$$

as one could have anticipated from (A26a). The optical transition amplitude, from (3.1), is, since $\epsilon(k_f)=\epsilon_k=-\epsilon(k_i)$,

$$\alpha^D_{c,v}(\omega)=An_{1,2}\frac{\xi_0}{L}\frac{\Delta_0}{\omega}\sum_k\frac{\Delta_0 2}{\epsilon_k^2}\delta(\omega-2\epsilon_k)\ .$$

Changing the sum to an integral using the appropriate (free) density of states gives

$$\alpha_D(\omega)=An_{1,2}\frac{\pi}{L}\frac{v_F}{\omega}\frac{L}{2\pi}\times\int dk\frac{\Delta_0^2}{k^2v_F^2+\Delta_0^2}\times\delta[\omega-2(k_0^2v_F^2+\Delta_0^2)^{1/2}]\ , \quad \text{(A34)}$$

which, upon integrating using the δ functions, yields the familiar result[18,20]

$$\alpha^D_{c,v}(\omega)=A\tfrac{1}{2}n_{1,2}\left[\frac{2\Delta_0}{\omega}\right]^2\frac{1}{(\omega^2-4\Delta_0^2)^{1/2}}\ . \quad \text{(A35)}$$

In the case of the kink, as a consequence of the particle-hole symmetry, the transitions involving the localized level at $\omega_0=0$ obey $\alpha^K_{c,0}=\alpha^K_{0,v}\equiv\alpha^0_K$ (the notation in the main text). To calculate α^0_K we use the kink results for the wave functions $f^0_\pm, f^{c,v}_{K\pm}$ as given by (2.7b) and (2.8).

From (A6) this yields

$$M^K_{0,v}=\frac{i}{2}\left[\frac{1}{\xi_0 L}\right]^{1/2}\int e^{iky}\mathrm{sech}\left[\frac{y}{\xi_0}\right]dy \quad \text{(A36a)}$$

or, using (A14a),

$$M^K_{0,v}=\frac{i}{2}\pi\left[\frac{\xi_0}{L}\right]^{1/2}\mathrm{sech}\left[\frac{\pi k\xi_0}{2}\right]\ . \quad \text{(A36b)}$$

Hence, going immediately to the continuum form,

$$\alpha^0_K=An_{1,2}\frac{\xi_0}{L}\frac{\Delta_0}{\omega}\frac{L}{2\pi}\int dk\left[\frac{\pi^2}{4}\frac{\xi_0}{L}\mathrm{sech}^2\left[\frac{\pi k\xi_0}{2}\right]\right]\delta(\omega-\epsilon_k)$$
$$=An_{1,2}\frac{\pi^2}{4}\frac{\xi_0}{L}\frac{1}{(\omega^2-\Delta_0^2)^{1/2}}\mathrm{sech}^2\left[\frac{\pi(\omega^2-\Delta_0^2)^{1/2}}{2\Delta_0}\right], \quad \text{(A37)}$$

which is the result quoted in the text.

The interband transition in the presence of the kink can be calculated in the same manner as for the polaron. Equation (A6) together with the appropriate wave functions $f^{c,v}_{K\pm}$ (2.8) yields

$$M^K_{c,v}=\frac{1}{2L}\frac{1}{(1+k^2\xi_0^2)^{1/2}(1+k'^2\xi_0^2)^{1/2}}(-i)\int_{-L/2}^{L/2}dy\,e^{i(k-k')y}\left\{(1+k^2\xi_0^2)^{1/2}\left[\tanh\left[\frac{y}{\xi_0}\right]+ik'\xi_0\right]\right.$$
$$\left.+(1+k'^2\xi_0^2)^{1/2}\left[\tanh\left[\frac{y}{\xi_0}\right]-ik\xi_0\right]\right\}$$
$$=\begin{cases}\dfrac{\xi_0}{L}\dfrac{\pi}{2}\left[\dfrac{1}{(1+k^2\xi_0^2)^{1/2}}+\dfrac{1}{(1+k'^2\xi_0^2)^{1/2}}\right]\dfrac{1}{\sinh[(\pi/2)(k-k')\xi_0]}\ , & k\neq k'\\ 0\ , & k=k'\end{cases} \quad \text{(A38)}$$

where we have used (A23a) again. We arrive at the same form for the matrix element as Kivelson *et al.*[18] *without* using the special boundary conditions for the kink. As discussed in the main text it is obvious from the k dependence of $M^K_{c,v}$ (A38) for $k-k'\to 0$ that special care has to be taken in summing over all k. Since this is done in detail elsewhere[18] we do not repeat it here. We want to stress that the kink boundary conditions are necessary *only* for the k integration, not for obtaining the matrix element (A38).

[1]W. P. Su, J. R. Schrieffer, and A. J. Heeger, Phys. Rev. Lett. 42, 1698 (1979); Phys. Rev. B 22, 2099 (1980).
[2]A. Kotani, J. Phys. Soc. Jpn. 42, 408 (1977); 42, 416 (1977).
[3]S. A. Brazoviskii, Zh. Eksp. Teor. Fiz. Pis'ma Red 28, 656 (1978) [JETP Lett. 28, 606 (1978)]; Zh. Eksp. Teor. Fiz. 78, 677 (1980) [Sov. Phys.—JETP 51, 342 (1980)].
[4]For reviews see *Physics in One Dimension,* edited by J. Bernasconi and T. Schneider (Springer, Berlin 1981); *The Physics and Chemistry of Low Dimensional Solids,* edited by L. Alcâcer (Reidel, Dordrecht, 1980); Proceedings of International Conference on Low-

Dimensional Synthetic Metals, Helsinger, Denmark, 1980 [Chem. Scr. 17, 1 (1981)].

[5]M. J. Rice, Phys. Lett. 71A, 152 (1979).

[6]E. J. Mele and M. J. Rice, Chem. Scr. 17, 21 (1981).

[7]N. Suzuki, M. Ozaki, S. Etemad, A. J. Heeger, and A. G. MacDiarmid, Phys. Rev. Lett. 45, 1209 (1980); *ibid.* 45, 1483(E) (1980).

[8]S. Etemad and A. J. Heeger, in *Nonlinear Problems: Present and Future,* edited by A. R. Bishop, D. K. Campbell, and B. Nicolaenko (North-Holland, Amsterdam, 1982), p. 209.

[9]A. Feldblum, J. Kaufman, S. Etemad, A. J. Heeger, T.-C. Chung, and A. G. MacDiarmid, Phys. Rev. B 26, 819 (1982).

[10]W. P. Su and J. R. Schrieffer, Proc. Natl. Acad. Sci. U. S. A. 77, 5526 (1980).

[11]J. L. Bredas, R. R. Chance, and R. Silbey, Mol. Cryst. Liq. Cryst. 77, 319 (1981).

[12]D. K. Campbell and A. R. Bishop, Phys. Rev. B 24, 4859 (1981).

[13]S. Brazovskii and N. Kirova, Zh. Eksp. Teor. Fiz. Pis'ma Red. 33, 6 (1981) [JETP Lett. 33, 4 (1981)].

[14]S. Etemad, A. Feldblum, A. J. Heeger, T.-C. Chung, A. G. MacDiarmid, A. R. Bishop, D. K. Campbell, and K. Fesser (unpublished).

[15]T.-C. Chung, A. Feldblum, A. G. MacDiarmid, and A. J. Heeger, J. Polym. Sci. Polym. Lett. Ed. (in press); A. Feldblum, A. J. Heeger, T.-C. Chung, and A. G. MacDiarmid, J. Chem. Phys. 77, 5114 (1982).

[16]L. Lauchlan, S. Etemad, T.-C. Chung, and A. J. Heeger, Phys. Rev. B 24, 1 (1981); J. Orenstein, and G. L. Baker, Phys. Rev. Lett. 49, 1043 (1982).

[17]A. J. Epstein (private communication).

[18]S. Kivelson, T.-K. Lee, Y. R. Lin-Liu, I. Peschel, and Lu Yu, Phys. Rev. B 25, 4173 (1982); B. Horovitz, Solid State Commun. 41, 593 (1982).

[19]Y. R. Lin-Liu, Phys. Rev. B 25, 5540 (1982).

[20]J. T. Gammel and J. A. Krumhansl, Phys. Rev. B 24, 1035 (1981).

[21]H. Takayama, Y. R. Lin-Liu, and K. Maki, Phys. Rev. B 21, 2388 (1980).

[22]B. Horovitz, Phys. Rev. Lett. 46, 742 (1981); Phys. Rev. B 22, 1101 (1980).

[23]D. K. Campbell and A. R. Bishop, Nucl. Phys. B 200, 297 (1982).

[24]R. F. Dashen, B. Hasslacher, and A. Neveu, Phys. Rev. D 12, 2443 (1975).

[25]P. G. de Gennes, *Superconductivity of Metals and Alloys* (Benjamin, New York, 1966); J. Bar-Sagi and C. G. Kuper, Phys. Rev. Lett. 28, 1556 (1972).

[26]W. P. Su, S. Kivelson, and J. R. Schrieffer, in *Physics in One Dimension,* edited by J. Bernasconi and T. Schneider (Springer, Berlin, 1981), p. 201.

[27]W. P. Su, Solid State Commun. 35, 899 (1980).

[28]This is a characteristic of the solitonic properties of the reflectionless potentials $\Delta_K(y)$ and $\Delta_P(y)$ in Eq. (2.3).

[29]W. P. Su and J. R. Schrieffer, Phys. Rev. Lett. 46, 738 (1981); R. Jackiw and J. R. Schrieffer, Nucl. Phys. B 190, 253 (1981).

[30]S. Brazoviskii, S. Gordyunin, and N. Kirova, Zh. Eksp. Teor. Fiz. Pis'ma Red. 31, 486 (1980) [JETP Lett. 31, 456 (1980)].

[31]This important result, which is again a consequence of the partial soliton nature of the problem, permits us to express the optical-absorption matrix elements analytically for any values of $K_0 v_F$ or ω_0. This will allow us, without separate calculations, to discuss optical absorption from polarons in *cis*-$(CH)_x$ (and perhaps other related polymers) since, at least in the model of Ref. 13, the same wave functions occur; only the value of $K_0 v_F$ (or ω_0) is different.

[32]K. Fesser, A. R. Bishop, and D. K. Campbell (unpublished). We also thank S. Kivelson for discussions on this point.

[33]A. R. Bishop, D. K. Campbell, and K. Fesser, Mol. Cryst. Liq. Cryst. 77, 253 (1981).

[34]A. R. Bishop and D. K. Campbell, in *Nonlinear Problems: Present and Future,* edited by A. R. Bishop, D. K. Campbell, and B. Nicolaenko (North-Holland, Amsterdam, 1982), p. 195.

[35]The same phenomenon appears in BCS theory of superconductivity where the ultrasonic and infrared absorptions show similar differences. We thank J.R. Schrieffer for drawing our attention to this important point. [See, e.g., J. Bardeen, L. Cooper, and J. R. Schrieffer, Phys. Rev. 108, 1175 (1957).]

[36]Y. Tomkiewicz *et al.*, in *Physics in One Dimension,* edited by J. Bernasconi and T. Schneider (Springer, Berlin, 1981), p. 214.

[37]Analytic forms for polaron lattice solutions in polymers with nondegenerate ground states can be obtained using the technique recently developed by S. Brazoviskii, I. Dzyaloshinski, N. Kirova, and I. Kirchever, Zh. Eksp. Teor. Fiz. 83, 389 (1982), and preprints. We thank Igor Dzyaloshinski for bringing this work to our attention.

[38]M. Nakahara and K. Maki, Phys. Rev. B 25, 7789 (1982).

[39]A. J. Heeger and A. G. MacDiarmid, in *The Physics and Chemistry of Low Dimensional Solids,* edited by L. Alcâcer (Reidel, Dordrecht, 1980).

[40]Contrast the mechanism here for confinement and recombination barriers with those typical in polaron-exciton theories from *e-e* interactions. [See, e.g., D. Emin, Phys. Today 35 (6), 34 (1982)].

[41]D. Bloor, F. H. Preston, and D. J. Ando, Chem. Phys. Lett. 38, 33 (1976).

[42]See, e.g., G. W. Bryant and A. J. Glick, J. Phys. C 15, L391 (1982).

[43]See the evidence from vibronic transitions, Ref. 14.

[44]D. Baeriswyl, G. Harbeke, H. Kiess, and W. Meyer, in *Electronic Properties of Polymers,* edited by J. Mort and G. Pfister (Wiley, New York, 1982), p. 267.

[45]See, e.g., L. D. Landau and E. M. Lifschitz, *Quantum Mechanics* (Pergamon, New York, 1977).